mac ltd
MULTIPLE ACCESS COMMUNICATIONS

A Study to Determine the Potential for Harmful Interference from TDD LTE Systems Operating in the 2300 – 2400 MHz Band into ZigBee Devices

Final Report

July 2013

MAC-EXFR-28-002

This report was commissioned by Ofcom

Version	Comments	Date
Version 0.1	Incomplete draft release to Ofcom	07-Jun-2013
Version 1.0	Initial release	17-Jun-2013
Version 1.1	Updated with feedback from Ofcom	10-Jul-2013
Version 1.2	Clarification of conclusions	18-Jul-2013

Executive Summary

A Study to Determine the Potential for Harmful Interference from TDD LTE Systems Operating in the 2300 – 2400 MHz Band into ZigBee Devices

Final Report

Background

Ofcom is currently examining the potential uses of the 2300 – 2400 MHz frequency band that is being released by the Ministry of Defence in the United Kingdom. Given the rising demand for broadband communications, one possible use is to support LTE systems in a time division duplex (TDD) arrangement. The band is directly adjacent to the unlicensed 2.4 GHz industrial, scientific and medical (ISM) band, which is used by a range of different local and personal area communications technologies such as WiFi, Bluetooth and ZigBee. Although systems operating within the ISM band do so on a non-interference, non-protection basis, it is still important for Ofcom to understand the impact on these systems of introducing new technologies into the 2300 – 2400 MHz band. To this end, Ofcom has commissioned Multiple Access Communications Limited (MAC Ltd) to perform a study into the impact of a TDD LTE system operating in the 2300 – 2400 MHz band on the performance of ZigBee systems operating in the adjacent ISM band. This study consists of a brief theoretical analysis of the performance of ZigBee devices based on published literature, followed by measurements performed on representative ZigBee devices. In this report we present the results of the theoretical analysis and also the results and conclusions from the measurement programme.

Theoretical Analysis

Ideally it would be possible to test application-specific ZigBee devices (eg, smart meters, lighting controllers, health monitors) and determine the manner in which they perform under different interference scenarios. However, the ZigBee specifications do not mandate a test mode for the purposes of making objective radio link measurements and, therefore, this was not a viable approach for our measurement programme. Instead we selected a number of development boards based on chipsets from leading ZigBee chipset manufacturers and these

were tested as part of our measurement programme. As part of our theoretical analysis, we identified the leading chipset manufacturers based on the presence of their products amongst the 60 ZigBee Compliant Platforms listed by the ZigBee Alliance. From this group we chose development boards based on chipsets from four vendors for the purposes of testing. We also tested a ZigBee device in a Universal Serial Bus (USB) 'stick' format based on a chipset from one of these vendors to understand the performance of devices with internal antennas. Finally we tested the performance of a ZigBee-based home automation system to understand the impact of introducing TDD LTE interference on a typical off-the-shelf system.

Our analysis of chipset performance data was inconclusive in determining whether the selectivity and blocking characteristics of the receivers or the out-of-band emissions (OOBEs) from the TDD LTE transmitters are likely to be the limiting factor in the performance of a ZigBee device. This aspect was investigated further in the measurement programme through the use of receiver blocking and OOBE tests.

Test Methodology

The set-up used for our measurements is shown in Figure A1. The 'wanted' ZigBee signal was generated from the transmitter of the development board, whereas the interference signals were generated using a signal generator. These two signals were combined and then fed simultaneously to the device under test (DUT) and a spectrum analyser. MATLAB scripts running on a PC were used for controlling the test equipment and for recording and analysing the measurement results.
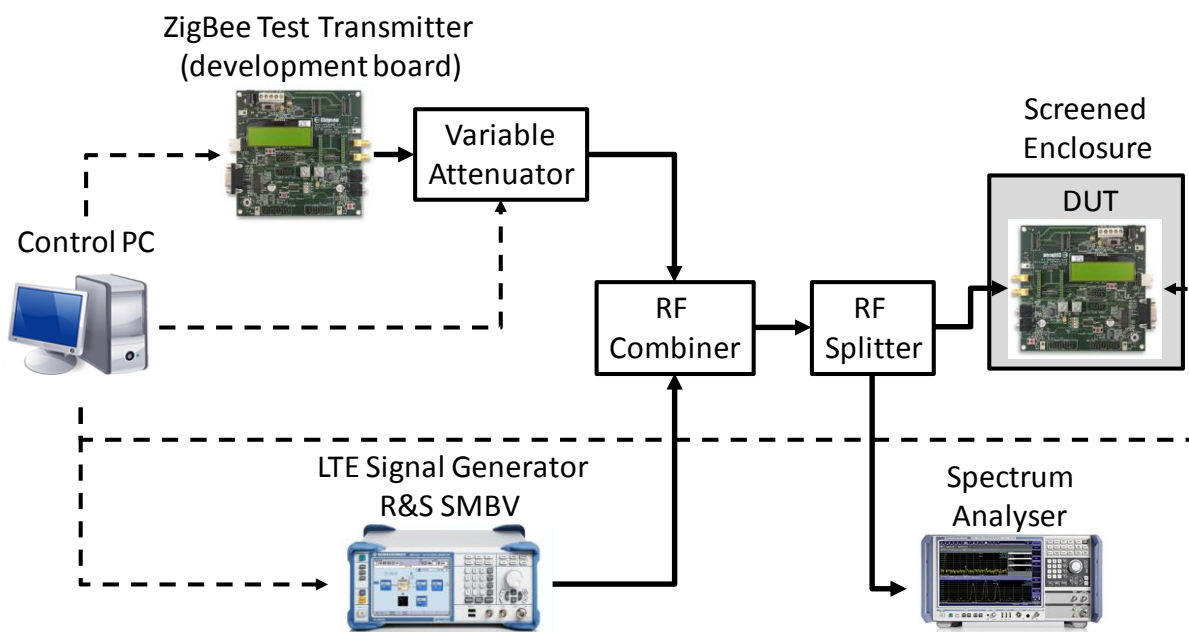
Figure A1 Test Set-up

The testing involved measuring the minimum carrier to interference ratio (C/I) needed to maintain a packet error rate (PER) of 1% on the ZigBee link in the presence of carrier wave (CW) or TDD LTE interference. The following steps were carried out in the MATLAB scripts for performing these tests:

- Measure the 'minimum useable sensitivity' (MUS) of the DUT by increasing the attenuation in the ZigBee signal path until the PER was reduced to the 1% level, which is the way in which receiver sensitivity is defined in the ZigBee standards. The transmit power of the ZigBee transmitter and the loss in the signal path were used to determine the signal level at the antenna connector of the DUT.

- The ZigBee signal strength was increased by 10 or 20 dB above the MUS.

- An interfering signal was introduced at the selected frequency offset and its power level was increased until the PER reduced to the 1% level. The C/I ratio at this point was recorded.

- This process was repeated for a range of frequency offsets and interfering signal types.

Ofcom provided MAC Ltd with examples of OOBE measurements for TDD LTE user equipments (UEs) operating in the 800 MHz band and LTE base stations (BSs) operating in the 2620 to 2690 MHz band. MAC Ltd used the arbitrary waveform functionality and the

associated signal libraries within the Rohde and Schwarz SMBV100A signal generator to produce signals that were representative of typical LTE UE and BS signals and these matched reasonably well with the measurement data provided by Ofcom. LTE Frame Configuration 5 was used as the primary downlink configuration, with the downlink slots containing the BS transmissions and with inactive uplink slots. Frame Configuration 3 was chosen as the primary uplink configuration, with the uplink slots containing UE transmissions and with downlink slots inactive.

Results

An example of LTE OOBE and CW blocking test results obtained in this study is shown in Figure A2 below. This particular example shows the target C/I values for this device in the presence of different types of interfering signals located at various frequency offsets relative to the ZigBee channel centre frequency of 2405 MHz (Channel 11). The ZigBee signal was given an uplift of 20 dB relative to the measured MUS of the DUT.
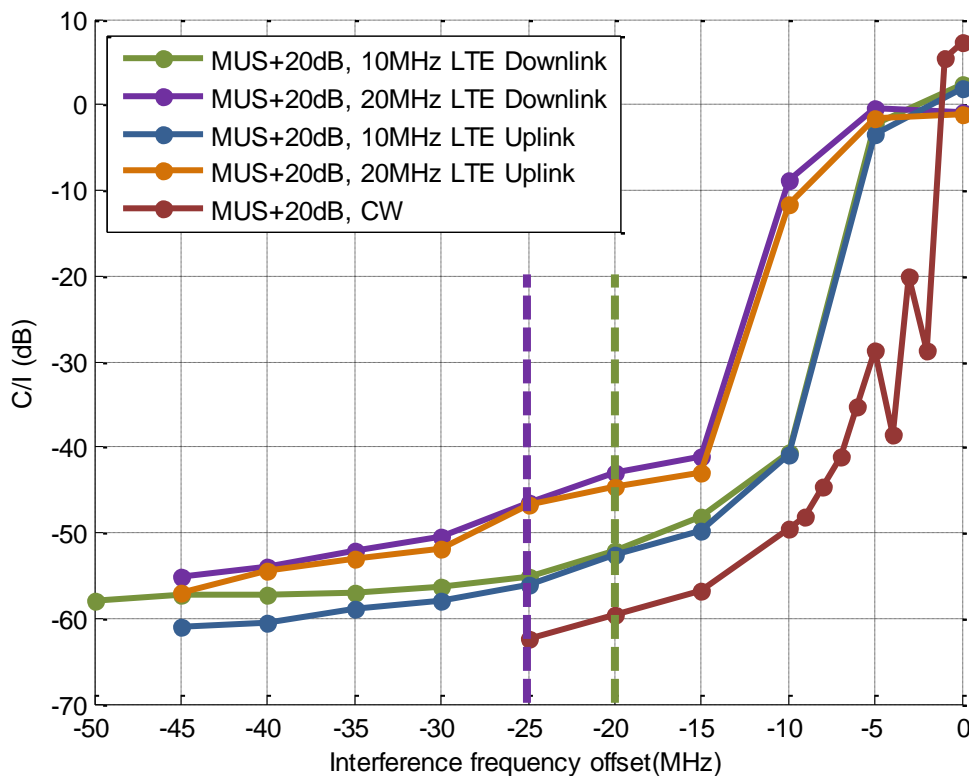
Figure A2   An example C/I measurement result. (MUS for this device was measured to be -92.1 dBm).

The results show that the effect of the interference decreases as the relative offset between the ZigBee and TDD LTE signals is increased. The CW curve (brown) drops more sharply compared to the TDD LTE curves. Furthermore, the 10 MHz TDD LTE curves (blue and green) drop to their minimum value more quickly compared to the 20 MHz TDD LTE curves (purple and orange). At a frequency offset of up to 5 MHz, the TDD LTE signals (of both 10 and 20 MHz bandwidth) cause significant interference to the ZigBee link. At a frequency offset of 10 MHz, the 10 MHz TDD LTE signal no longer overlaps the ZigBee signal, and the target C/I drops sharply. However, the 20 MHz TDD LTE signal takes a much larger frequency offset for its target C/I curves to drop to their minimum value. According to Ofcom's proposed channel plan for the 2300 – 2400 MHz band, the centre frequency of the upper 20 MHz bandwidth channel will be 2380 MHz (ie, an offset of -25 MHz in the figure, shown with a purple vertical dashed line) and for the upper 10 MHz bandwidth channel it will be 2385 MHz (ie, an offset of -20 MHz in the figure, shown with a green vertical dashed line).

We chose LTE Frame Configuration 5 and an output spectrum with a low OOBE for the downlink interference and Frame Configuration 3 with a higher OOBE for the uplink. The effects of downlink and uplink interference are generally quite similar. We expected that due to a higher transmission duty cycle, the Frame Configuration 5 used in the downlink TDD LTE interferer would cause a slightly higher level of disruption compared to Frame Configuration 3, which was used for the uplink. However, we also expected that this may be compensated due to the greater OOBEs on the uplink spectrum. Our measurements show that this is indeed the case, and no clear trend is observed as to which type of interference (ie, uplink or downlink) causes more link degradation.

Figure A3 shows the variation in target C/I when the uplift level in the ZigBee signal is changed from 10 dB to 20 dB. An increase of 10 dB is required for the CW interference signal to counteract a 10 dB increase in ZigBee signal uplift, resulting in an unchanged target C/I. However, an increase of only about 3 dB is needed to counteract this change in the case of the 20 MHz TDD LTE interferer, resulting in the target C/I curves (purple) shifting upwards by approximately 7 dB. This suggests the presence of intermodulation products caused by non-linear distortion in the ZigBee receiver.
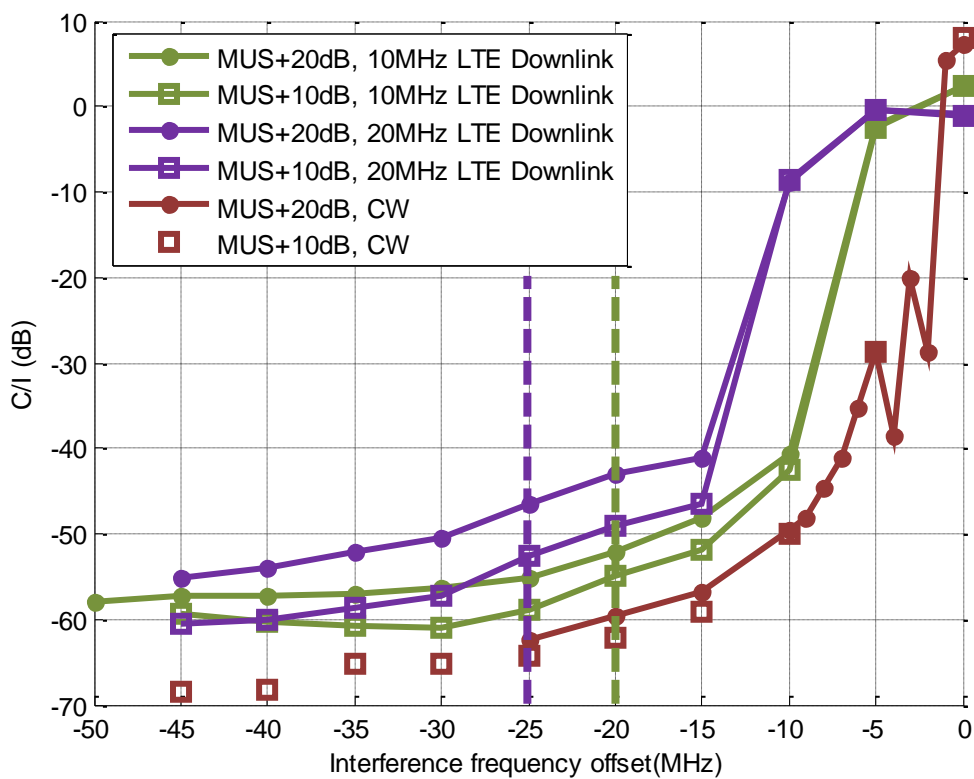
Figure A3   Comparison of target C/I with varying levels of ZigBee signal uplift. This device showed evidence of non-linearities during interference testing. (MUS = -92.1 dBm)

Another example of the C/I measurement results for a different device is shown in Figure A4. In this case, the target C/I is unchanged when the ZigBee signal uplift level is changed from 10 dB to 20 dB above MUS. This suggests that the receiver is not showing non-linear behaviour in the presence of high levels of interference and intermodulation products are not the dominant mechanism causing the desensitisation of the ZigBee receiver. Instead the receiver is being desensitised by the presence of the interfering signal at its front end, possibly through a decrease in the receiver gain caused by the automatic gain control mechanism (AGC) and, as a result, the device is not being driven into its non-linear region of operation. Therefore, we see no difference between the impact of narrow band and wide band interferers.
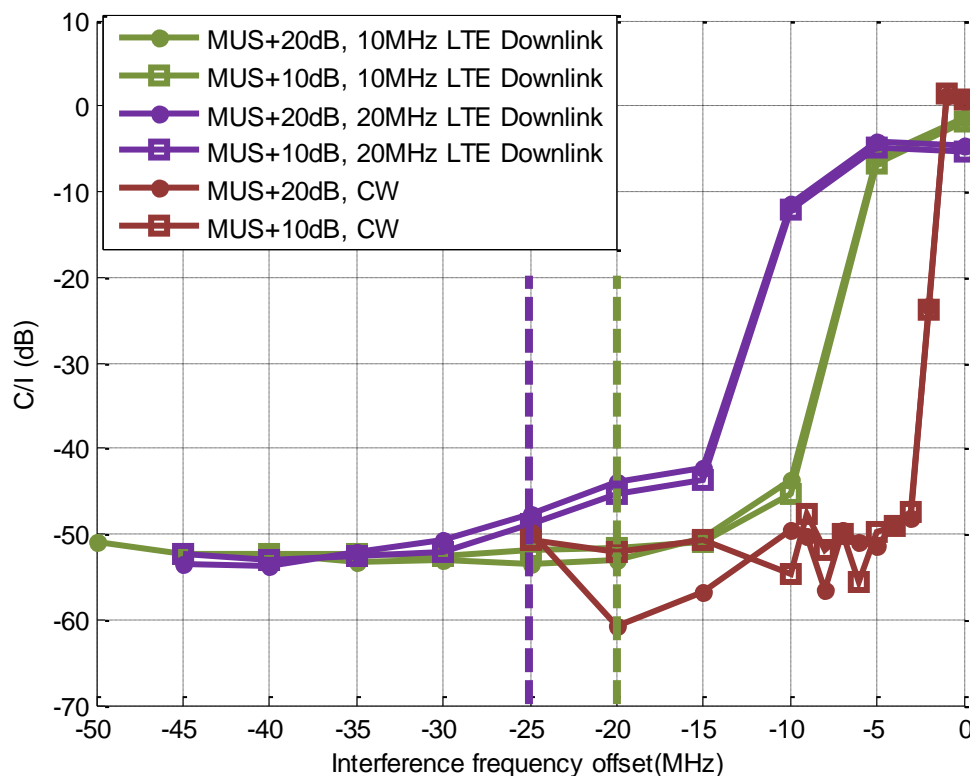
Figure A4 Example of measurement results from a ZigBee device that did not exhibit non-linear behaviour during interference testing. (MUS for this device was measured to be -95.3 dBm).

Based on the target C/I results obtained in our measurements, we calculated the minimum coupling loss (MCL) and minimum separation distance (MSD) needed for each of the devices to operate at a 1% PER in the presence of TDD LTE interference. These calculations were conducted for two scenarios. In the first case, a TDD LTE UE was considered as the source

of interference and a free-space model was used to calculate the path loss. The range of MSDs for the devices tested in our study was found to be 1.4 to 4.0 metres and 2.8 to 7.9 metres in case of 10 MHz and 20 MHz TDD LTE interferers, respectively. In the second scenario, a TDD LTE BS was considered as the source of interference. A free-space path loss model was used for distances of less than 50 m and a fourth-order path loss model was used for distances of greater than 50 m. The range of MSDs in this case was found to be 93.7 to 155.2 metres and 156.4 to 255.0 metres for 10 MHz and 20 MHz TDD LTE interferers, respectively. In both cases, we found that the devices with the lowest MUS values needed the highest MSD from the TDD LTE equipment.

We also conducted a set of protocol tests on one of the devices. In these tests, we enabled the packet reliability mechanisms such as packet acknowledgment and retransmissions as well as the carrier sense multiple access with collision avoidance (CSMA-CA) channel access mechanism. We found that this ZigBee device was able to cope well with high levels of interference, but the net data rate achieved by the ZigBee link dropped as the ZigBee signal strength (and consequently, the C/I) was decreased. Figure A5 shows the performance of an example when frame acknowledgment, frame retransmission and CSMA-CA are enabled.

We also tested the operation of a ZigBee-based home automation system in the presence of TDD LTE interference centred at the channels closest to the ISM band. These products comprised a central control panel, a mains relay and a remote control. We found that the presence of the TDD LTE interference at the maximum transmitted power of a UE had no measurable impact on the operation of these devices.
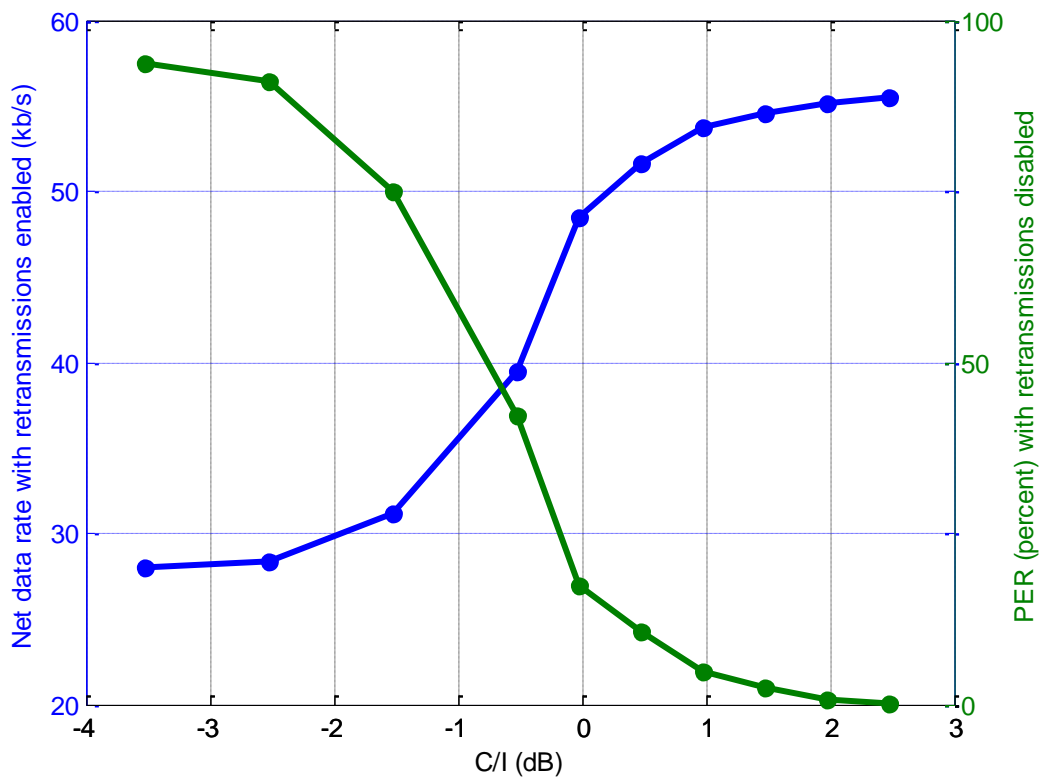
Figure A5   Net data rate as a function of C/I with frame retransmissions enabled in the presence of 10 MHz downlink TDD LTE interference. Also shown is the PER with retransmissions disabled.

Conclusions

Our overall conclusion is that the operation of TDD LTE equipment in the vicinity of the 2.4 GHz ISM band is unlikely to cause significant disruption to the operation of typical ZigBee devices available in the market that are being used in low data rate and non real time applications at a significant link margin (eg, >20 dB) above the minimum useable sensitivity for the particular system. Although the 'raw' performance of the ZigBee link could be adversely affected by interference from TDD LTE equipment, this is likely to be compensated by mechanisms within the ZigBee protocol stack such as frame retransmission and CSMA-CA. However, system performance issues could arise if the ZigBee equipment is operated in close proximity to a high power TDD LTE BS.

Prepared by Multiple Access Communications Ltd

July 2013

Table of Contents

List of Abbreviations

3GPP	Third Generation Partnership Project
ACR	Adjacent channel rejection
AL	Application layer
AM	Amplitude modulation
AODV	Ad hoc On-Demand Distance Vector
APS	Application support
BAW	Bulk acoustic wave
BS	Base station
CCA	Clear channel assessment
CIR	Carrier-to-interference ratio
CMOS	Complementary metal-oxide silicon
CSMA-CA	Carrier sense multiple access with collision avoidance
CW	Carrier wave
DC	Direct current
DL	Downlink
DSSS	Direct sequence spread spectrum
DUT	Device under test
ED	Energy detection
ETSI	European Telecommunications Standards Institute
EVM	Error vector magnitude
FDMA	Frequency division multiple access
HVAC	Heating, ventilation, and air conditioning
IEEE	Institute of Electrical and Electronics Engineers
IF	Intermediate frequency
IP	Internet protocol
ISM	Industrial, scientific and medical

KVP	Key value pair
LTE	Long term evolution
MAC	Medium access control
MCL	Minimum coupling loss
MSD	Minimum separation distance
MUS	Minimum useable sensitivity
NWK	Network (layer)
OFDMA	Orthogonal frequency division multiple access
OOB	Out-of-band
OOBE	Out-of-band emission
PAN	Personal area network
PEP	Peak envelope power
PER	Packet error rate
PHY	Physical (layer)
PN	Pseudo-noise
PSD	Power spectral density
PSSS	Parallel sequence spread spectrum
QAM	Quadrature amplitude modulation
QPSK	Quadrature phase shift keying
RF	Radio frequency
RF4CE	Radio frequency for consumer electronics
SAW	Surface acoustic wave
SC-FDMA	Single-carrier frequency division multiple access
SIR	Signal-to-interference radio
SNR	Signal-to-noise ratio
TDD	Time division duplex
UE	User equipment

UL   Uplink

ZDO   ZigBee device object

1 Introduction

Ofcom is currently examining the impact on ZigBee devices of any future decision to permit the use of Time Division Duplex (TDD) Long Term Evolution (LTE) equipment in the 2300-2400 MHz frequency band. Ofcom's plan for the release band of 2350 MHz to 2390 MHz is shown in Figure 1 for 20 MHz TDD LTE transmissions. In the case of 10 MHz TDD LTE transmissions, the centre frequency of the uppermost channel will be 2385 MHz. There is concern that TDD LTE equipment operating in this frequency band may have a detrimental impact on ZigBee devices operating in the neighbouring industrial, scientific and medical (ISM) band. Despite operating in a band that offers no guarantee of protection from interference, this is not a fact that would be understood by most consumers and so, before allocating the spectrum, Ofcom wishes to understand if TDD LTE devices pose a significant problem and if so what steps can be taken to minimise any interference they would cause. For this reason, Ofcom has commissioned Multiple Access Communications Limited (MAC Ltd) to conduct a study consisting of a brief theoretical analysis of the likely impact of adjacent band LTE services on ZigBee receivers and a programme of laboratory-based measurements to support the theoretical analysis. This report contains the results of the theoretical analysis and the results and conclusions of the laboratory testing.
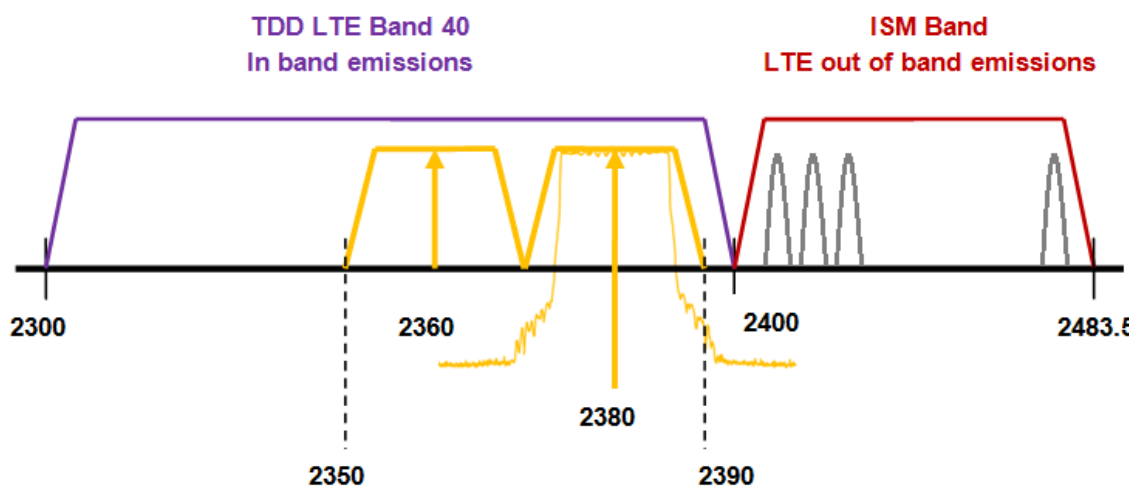
Figure 1   Plan for release band.

The impact of LTE equipment operating in an adjacent band on users of ZigBee systems depends on a number of factors such as the out-of-band (OOB) spectrum characteristics of interfering LTE signals, the ZigBee radio receiver performance, the ZigBee protocol stack

parameter settings and the quality of service requirements of ZigBee applications. In this report we start by examining the out-of-band spectrum characteristics of the LTE system in Section 2. Following a brief overview of the ZigBee standard in Section 3, we present an analysis of the interference rejection capability of ZigBee receivers in Section 4. Various interference mitigation mechanisms and their effectiveness are discussed in Section 5. A detailed description of the laboratory-based measurements is presented in Section 6 and the results of this testing are presented in Section 7. An analysis of the test results are presented in Section 8 and these results are used to calculate the minimum coupling loss and minimum separation distances between TDD LTE and ZigBee devices in Section 9. The impact of different aspects of the ZigBee protocol is explored in Section 10 and the testing of an off-the-shelf ZigBee-based home automation system is presented in Section 11. Finally, our conclusions are presented in Section 12.

2 TDD LTE Signal Characteristics

TDD LTE systems can operate in a range of channel bandwidths with 10 MHz and 20 MHz being the most likely options for the 2300 – 2400 MHz frequency band. For the purposes of this project, the important aspects of the TDD LTE system are those that have an impact on the characteristics of the uplink and downlink transmitted signal and, hence, the interference that will be experienced by ZigBee devices operating in an adjacent frequency band. The TDD LTE system uses the orthogonal frequency division multiple access (OFDMA) scheme on the downlink and the single carrier frequency division multiple access (SC-FDMA) scheme on the uplink. The SC-FDMA scheme requires a more complex receiver at the base station (BS), but it produces a lower peak-to-average power ratio, which relaxes the performance requirements of the transmitter at the user equipment (UE). Despite the difference in the names, these schemes are very similar in terms of the transmitted signals that are generated. In both schemes the multiple access element is provided by assigning different sub-carriers (or resource blocks) within the transmitted signal to different UEs. Three different modulation schemes are available for use in TDD LTE on both the uplink and the downlink, namely, quadrature phase shift keying (QPSK), 16-level quadrature amplitude modulation (16QAM) and 64QAM.

TDD LTE allows a flexible allocation of uplink and downlink resources in terms of the number of time slots allocated in each direction as shown in Table 1. The uplink and downlink time slot allocation can be changed in real time in response to changes in demand.

The 10 ms radio frame consists of 10 sub-frames of 1 ms duration and these can be assigned to the uplink (U) or the downlink (D). A further special sub-frame (S) is used to mark the transition between downlink and uplink sub-frames. The periodicity with which the downlink to uplink switch occurs can be either 5 ms (Configurations 0 to 2 and 6) or 10 ms (Configurations 3 to 5).

Uplink/Downlink Configuration	Downlink to Uplink Switching Period (ms)	Sub-frame									
		0	1	2	3	4	5	6	7	8	9
0		D	S	U	U	U	D	S	U	U	U
1	5	D	S	U	U	D	D	S	U	U	D
2		D	S	U	D	D	D	S	U	U	D
3		D	S	U	U	U	D	D	D	D	D
4	10	D	S	U	U	D	D	D	D	D	D
5		D	S	U	D	D	D	D	D	D	D
6	5	D	S	U	U	U	D	S	U	U	D

Table 1 LTE frame structure and permitted configurations (D=downlink, U=uplink and S=special).

The switching between uplink and downlink sub-frames means that TDD LTE transmissions are discontinuous, which is potentially more disruptive to other radio systems in adjacent frequency bands. This is because the pulsing can be seen as 100% amplitude modulation (AM) and is easily demodulated by any non-linearity in a receiver and the AM spectrum imposed on TDD LTE signals raises the OOBE levels compared to a continuous signal with the same underlying modulated spectrum.

3   Overview of the ZigBee Standard

The ZigBee specifications are a set of high level communication protocols produced by the ZigBee Alliance for small, low power digital radios based on the IEEE 802.15.4 standard. The overall protocol stack architecture of the core ZigBee specification [1] is illustrated in Figure 2 and it consists of a network layer (NWK) and a framework for application layer defined by the ZigBee Alliance on top of the medium access control (MAC) layer and physical (PHY) layer defined in the IEEE 802.15.4 specification [2].
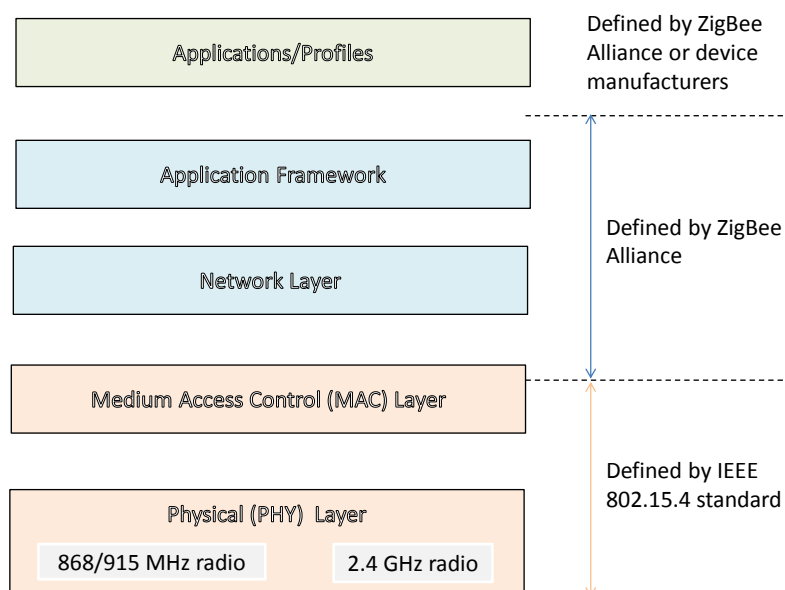
Figure 2   Outline of ZigBee stack architecture.

The key features of each protocol layer are briefly described below:

- **IEEE 802.15.4 PHY** offers a total of 27 channels with one in the 868 MHz band (868.0 – 868.6 MHz), 10 in the 915 MHz band (902 – 928 MHz) and 16 in the 2.4 GHz band (2400 – 2483.5 MHz). The bandwidth of these channels is approximately 600 kHz in the 868 MHz band and 2 MHz in the 915 MHz and 2.4 GHz bands. Note that according to the current frequency band allocation [3], only the 868 MHz and 2.4 GHz PHY layers can be used in the UK as the 915 MHz band is not available for unlicensed use. The raw bit rates available in the 868 MHz, 915 MHz and 2.4 GHz frequency bands are 20 kb/s (optional 100 kb/s and 250 kb/s), 40 kb/s (optional 250 kb/s) and 250 kb/s, respectively. Either direct sequence spread spectrum (DSSS) or parallel sequence spread spectrum (PSSS) is used, but no frequency hopping. In the 2.4 GHz frequency band, only DSSS is used. A physical packet consists of a synchronisation header, a physical header of one byte and a variable payload that can contain a maximum of 127 bytes.

- **IEEE 802.15.4 MAC** is a carrier sense multiple access with collision avoidance (CSMA-CA) medium access system with optional time slot structure and security functionality. It supports a star as well as a peer-to-peer network topology. The MAC

protocols in IEEE 802.15.4 can operate in both beacon-enabled and non-beacon modes. In the beacon-enabled mode, all communications are performed in a superframe structure. A superframe is bounded by periodically transmitted beacon frames, which allow devices to synchronise to the network. A superframe consists of an active part and an optional inactive period over which devices can go to sleep. The beacon-enabled mode is suitable for applications where power consumption must be kept particularly low. In the non-beacon mode, there is no time slot structure with which devices can synchronise and a device can transmit at any time based on CSMA-CA. This requires the constant reception of possible incoming data by at least some ZigBee devices.

- **ZigBee network layer (NWK)** is designed to provide functionality to ensure correct operation of the IEEE 802.15.4 MAC layer, efficient routing of packets within the network in a secure manner and a suitable service interface to the application layer.

- **ZigBee application layer (AL)** consists of the application support sub-layer (APS), ZigBee device objects (ZDO) and manufacturer defined application objects. The APS provides an interface between the application layer and the network layer.

There are two versions of the IEEE 802.15.4 specification: Release 2003 and Release 2006. The original 2003 version of the IEEE 802.15.4 standard specified a MAC layer and three PHY layers operating in the 868 MHz, 915 MHz and 2.4 GHz frequency bands. The 2006 version of the IEEE 802.15.4 standard introduced new modulation schemes for radios operating in both the 868 MHz and 915 MHz frequency bands and some enhancements to simplify the operation of the MAC layer. The 2006 specification is backwards-compatible with the 2003 specification, ie, devices conforming to the 2006 standard are capable of joining and functioning in a personal area network (PAN) composed of devices conforming to IEEE 802.15.4-2003. The ZigBee standard is based on the 2003 version of the IEEE 802.15.4 standard and for this study, we are only interested in devices operating in the 2.4 GHz frequency band.

There have been four releases of the ZigBee specifications. The first release is called ZigBee 2004, which is now more or less obsolete. The second release is called ZigBee 2006, and mainly replaces the message (MSG) frame and key value pair (KVP) frame structure used in the 2004 version with a 'cluster library'. The third release is called ZigBee 2007 and it

contains two stack profiles: Stack Profile 1 (simply called ZigBee) for home and light commercial use and Stack Profile 2 (called ZigBee PRO), which offers more features. The key differences between ZigBee and ZigBee PRO are as follows.

- The ZigBee feature set provides tree addressing, Ad hoc On-Demand Distance Vector (AODV) mesh routing, unicast, broadcast and group communication, security, etc

- ZigBee PRO replaces tree addressing with stochastic addressing, which scales better than tree addressing. It includes the same AODV routing but provides many-to-one source routing as an alternative. Both ZigBee and ZigBee PRO support group addressing, but PRO adds support for limited broadcast group addressing, which prevents unnecessary flooding of the entire network when all group members are in relatively close proximity. ZigBee PRO also adds support for 'high' level security, which provides a mechanism for establishing link keys between peer-to-peer connections, and adds additional security when devices on a network may not be trusted at the application layer.

The latest core ZigBee specification, officially named ZigBee 2012, offers full wireless mesh networking with ZigBee PRO and an optional new feature, known as Green Power, to connect energy harvesting or self-powered devices into ZigBee PRO networks.

In addition to the core ZigBee specification described above, there are also two additional specifications from the ZigBee Alliance, known as the ZigBee IP specification and the ZigBee RF4CE specification.

- The ZigBee IP specification [4] is an open standard for an IPv6-based full wireless mesh networking solution and provides seamless Internet connections to control low-power, low-cost devices. It was designed to support the ZigBee Smart Energy Version 2 standard.

- The ZigBee RF4CE specification [5] was designed for simple, two-way device-to-device control applications that do not require the full-featured mesh networking capabilities offered by the ZigBee specification.

A ZigBee application can be designed using the appropriate protocol stack defined in one of the above three ZigBee specifications (ie, ZigBee, ZigBee IP or ZigBee RF4CE). To ensure

the interoperability of equipment from different vendors within the same application space, the ZigBee Alliance has defined a list of ZigBee application standards for generically useful applications, known as ZigBee standard application profiles or public profiles. Each application profile is a description of the devices supported for the specific application, together with the messaging scheme used by those devices for communication. The ZigBee standard application profiles and the underlying specifications on which they are based are summarised in Table 2.

Profile name	Underlying Specification	Application domain
ZigBee Building Automation	ZigBee	Lighting, closures, Intruder Alarm Systems and some aspects of HVAC
ZigBee Remote Control	ZigBee RF4CE	Consumer electronics (CE) remote control (RC)
ZigBee Smart Energy	ZigBee	Metering, pricing and demand response and load control
ZigBee Health Care	ZigBee	Disease management, personal fitness/wellness monitoring
ZigBee Home Automation	ZigBee	Lighting, HVAC (heating, ventilation, and air conditioning), window shades and security
ZigBee Input Device	ZigBee RF4CE	For human interface devices (HIDs) such as keyboards to communicate with a host such as a PC
ZigBee Light Link	ZigBee	Consumer lighting
ZigBee Telecom services	ZigBee	Information delivery, location based services, peer-to-peer small data sharing, mobile commerce, mobile gaming, voice over ZigBee and chatting
ZigBee Gateway	ZigBee	Connection of ZigBee networks to Internet

Table 2   ZigBee standard application profiles.

Equipped with this basic knowledge of the ZigBee protocol stack specifications and application standards, we will now examine mechanisms available within ZigBee devices for mitigating the impact of radio interference.

4   Interference Rejection Capability

The first defence against interference for any radio system is to reject as much of the interfering signal as possible before it enters the receiver chain. This can be achieved by having a band-pass filter with a good selectivity at the front end of the receiver. It is also important to have a low noise amplifier with a good linearity characteristic to prevent spectral re-growth within the receiver front-end. However, high performance band-pass filters and amplifiers in this area often require bulky components resulting from the use of technologies such as surface acoustic wave (SAW) or bulk acoustic wave (BAW). Since the primary requirements for ZigBee chipsets are small size, low cost and low power consumption, a

technology based on the complementary metal-oxide silicon (CMOS) process is the preferred choice for the following reasons.

- CMOS provides unparalleled digital processing capability, enabling flexible and efficient implementation of the baseband signal processing.

- CMOS offers the benefit of low cost coupled with single-chip integration capability. Namely, it enables the integration of digital baseband processing, radio frequency (RF)/analogue circuits and system memory in the same physical silicon.

The drawback with the CMOS-based approach for an integrated RF and baseband radio-on-chip solution is that the filter rejection, noise performance and amplifier linearity are not as good as traditional heterodyne receivers. The radio-on-chip solution requires pushing the on-chip channel filtering function to lower frequencies through the use of single-conversion architectures, ie, the zero-intermediate frequency (zero-IF) and low-IF receiver architectures. The zero-IF receiver architecture has the problems of direct current (DC) offset and 1/f-noise. The low-IF receiver architecture overcomes the problems of DC offset and 1/f-noise, but re-introduces the image frequency issue, which is eliminated in zero-IF architectures. Fortunately, the requirement of the IEEE 802.15.4 standard on the image and adjacent channel rejection are relatively relaxed, making the CMOS radio-on-chip or system-on-chip an ideal choice for ZigBee chipset vendors. However, in the presence of a strong signal in an adjacent frequency band like a TDD LTE transmission, the compromised filter and amplifier performances are likely to be a problem as discussed below.

The radio transceiver performance in the 2.4 GHz frequency band defined in the IEEE 802.15.4 standard is summarised in Table 3. It can be seen that the specification requires that the receiver should have a sensitivity level of at least -85 dBm and should be able to receive a signal level of at least -20 dBm before saturation. Co-channel rejection is not specified, but with the modulation/spreading scheme used by 2.4 GHz IEEE 802.15.4 devices, a co-channel rejection of -5 dB or -6 dB (or a co-channel carrier-to-interference ratio of 5 dB or 6 dB) could be possible. The adjacent channel rejection (ACR) specification is illustrated in Figure 3, which suggests that for an IEEE 802.15.4 standard compliant radio, the receiver sensitivity would be degraded by 3dB if there is an interfering ZigBee signal 5 MHz away with a power level of -82 dBm or 10 MHz away with a power level of -52 dBm.

Parameter	Value
Number of channels	16
Channel spacing	5 MHz
Spectrum spreading	Direct spectrum spreading scheme (DSSS)
Chip modulation scheme	O-QPSK
Data rate	250 kb/s
Symbol rate	62.5 ksymbols/s
Chip rate	2 Mchips/s
Transmit characteristics	
- Output power	Capable of at least -3dBm
- Modulation accuracy	EVM < 35%
- Transmit power spectral density (PSD) mask	< -20 dB (relative limit) or < -30 dBm (absolute limit) for |f-fc|>3.5 MHz
Receive characteristics	
- Sensitivity	-85 dBm @ 1% PER
- Receiver maximum input level	-20 dBm
- Adjacent channel Rejection (ACR)	0 dB with desired signal at -82 dBm
- 2nd ACR	30 dB with desired signal at -82 dBm

Table 3   IEEE 802.15.4 specification for PHY at 2.4 GHz frequency band.
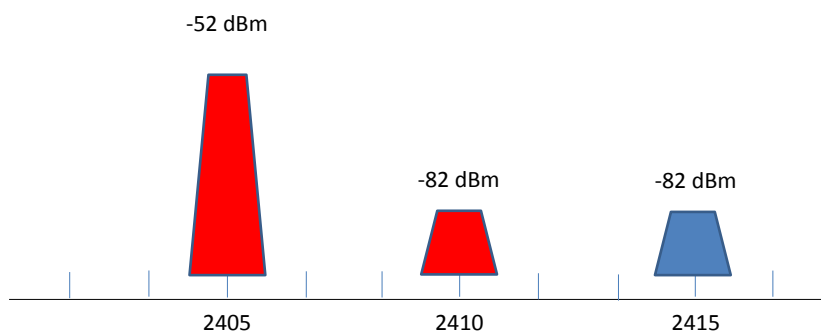
Figure 3   Illustration of ACR specification, where the wanted ZigBee signal is located at 2415 MHz.

The performance specified in IEEE802.15.4 provides a lower bound. The actual radio receiver performance is often better than the specification. To gain an insight into the actual radio receiver performance of ZigBee devices available on the market, we require some

information on the radio chipsets used in ZigBee products. There are thousands of certified ZigBee products from over hundreds of different manufacturers. It has not been possible within the scope of this project to investigate the full range of ZigBee products that are available to determine the radio chipsets used. Besides, such information is often omitted from the publically available product descriptions. Therefore, we have taken the following approach to establish an indication of the main ZigBee radio chipsets that are in deployment.

According to the ZigBee Alliance, ZigBee compliant platforms are the foundation of all ZigBee products. Each platform is comprised of a 2.4 GHz radio and a microprocessor, with storage, running the ZigBee firmware. At the time this report was compiled, there were a total of 60 ZigBee compliant platforms published on the ZigBee Alliance website (www.zigbee.org). Of these platforms, the radio chipsets used are distributed among the ZigBee chipset vendors as shown in Figure 4.
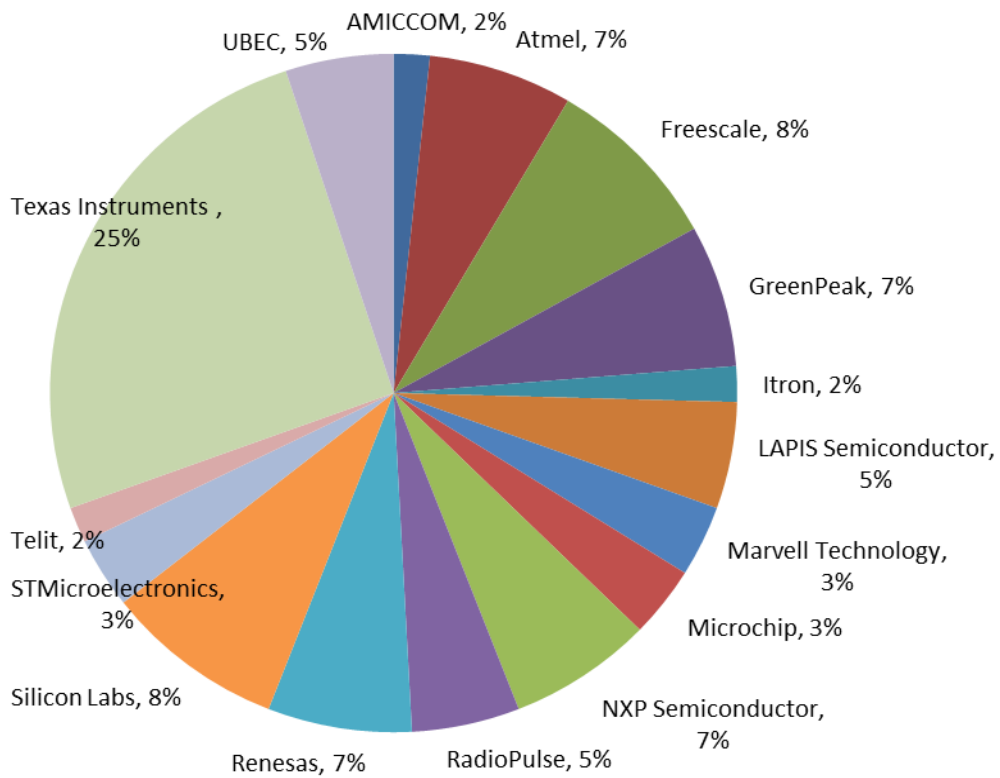
Figure 4   Chipset vendor distribution across the ZigBee compliant platforms.

We examined the receiver performance of example radio chipsets supplied by some of the manufacturers listed in Figure 4, and the results are presented below.

Vendor	TI	Freescale	Silicon Labs	Atmel
Model	CC2530 [6]	MC1322x [7]	EM351/357 [8]	AT86RF233 [9]
Sensitivity (dBm)	-97	-100	-100	-101
Max Input Level (dBm)	10	10	0	8
Co-channel rejection (dB)	-3		-6	
ACR at -5 MHz/+5 MHz (dB)	49/49	38/38	47/39	32/35
ACR at -10 MHz/+10 MHz (dB)	57	57/57	49/49	48/48
ACR at -15 MHz/+15 MHz (dB)		65	40	54/54
ACR at <= -20 MHz and >=+20 MHz (dB)	57		40	

Table 4   Receiver performance of some chipsets on the market.

Compared against the performance defined in the IEEE 802.15.4 standard, the sensitivity levels of these chipsets are better by at least 12 dB, whilst saturation levels are at least 20 dB higher. The adjacent channel rejection performances of these chipsets are also well above the specified values. Taking the MC1322x chipset from Freescale as an example, its adjacent channel rejection is 38 dB better than required by the IEEE 802.15.4 standard and its alternate channel rejection is 27 dB better than required by the standard. We also note that the adjacent channel rejection capability varies from chipset to chipset. For example, at -5 MHz away from the wanted signal frequency, the CC2530 from TI claims a 49 dB rejection and the AT86RF233 from Atmel claims a 32 dB rejection, giving a difference of 17 dB.

In order to assess the potential performance of a ZigBee receiver in the face of interference from a neighbouring TDD LTE interfering signal, let us start by considering the performance of a ZigBee receiver with a perfect channel filter, ie, a channel filter that provides infinite attenuation to signals that lie outside of a 2 MHz band that is centred on the ZigBee channel. Based on the TDD LTE OOBEs and spurious emissions limits for the UE defined in the 3GPP standards [10], if a 10 MHz TDD LTE transmission is centred on 2385 MHz (ie, the upper 10 MHz channel of the band to be released), then the power at the lowest ZigBee channel (Channel 11[1]), centred at 2405 MHz, will be -25 dBm measured in the lower 1 MHz

---

[1] The ZigBee channel plan in the 2.4GHz frequency band consists of 16 channels spaced at 5 MHz intervals centred at 2405 MHz to 2480 MHz and numbered from Channel 11 (2405 MHz) to Channel 26 (2480 MHz).

of the 2 MHz receiver bandwidth and -30dBm in the upper 1MHz of the receiver bandwidth, which corresponds to a power of around -24 dBm in the full 2 MHz ZigBee receiver bandwidth. Taking the TI CC2530 device in Table 4 as an example, its co-channel rejection ratio is -3 dB, which means that it will operate at its reference sensitivity performance with a wanted received ZigBee signal of -82 dBm and a co-channel interfering signal of -85 dBm. If we assume that the TDD LTE OOBEs have the same performance impact as a co-channel ZigBee signal, then this means that the minimum coupling loss (MCL) that can be tolerated between the TDD LTE transmitter and the TI CC2530 receiver is 61 dB when the desired signal received is at -82 dBm.

Having examined the MCL for a ZigBee receiver with perfect selectivity, let us examine the performance of a practical ZigBee receiver in the face of interference from a TDD LTE transmitter with perfect OOBE performance, ie, the TDD LTE transmitter does not generate any emissions outside of its channel bandwidth. This performance is governed by the blocking characteristic of ZigBee receivers. Unfortunately, the blocking performance is not specified by the IEEE 802.15.4 standard. Consequently, not all the chipset vendors provide information on receiver blocking performance. Among the four ZigBee chipsets in Table 4, only the CC2530 and the EM351/EM357 datasheets include blocking performance. We will again take the CC2530 from TI as an example, assuming that, in a competitive market, the chipsets from other vendors will have similar performance. The blocking performance, which is measured at a given frequency offset from the band edge, for the CC2530 radio receiver is shown in Figure 5. The performance is measured with a wanted signal 3 dB above the sensitivity level of -85 dBm and a carrier wave (CW) interferer, with a reference performance of a 1% packet error rate (PER).

Figure 5 shows that a CW interferer at -35 dBm received at 2390 MHz will cause a 3 dB degradation in the performance of the ZigBee receiver. If we assume that a TDD LTE transmitter at 2385 MHz will have a similar impact on the performance of the ZigBee receiver, then a MCL of 58 dB is required to protect the ZigBee receiver in this example, assuming that the TDD LTE transmitter is a UE with transmit power of 23 dBm. However, the blocking performance of receivers with regards to wideband signals tends to be worse than that measured with CW signals, so we would expect the MCL to be greater for a TDD LTE transmitter.
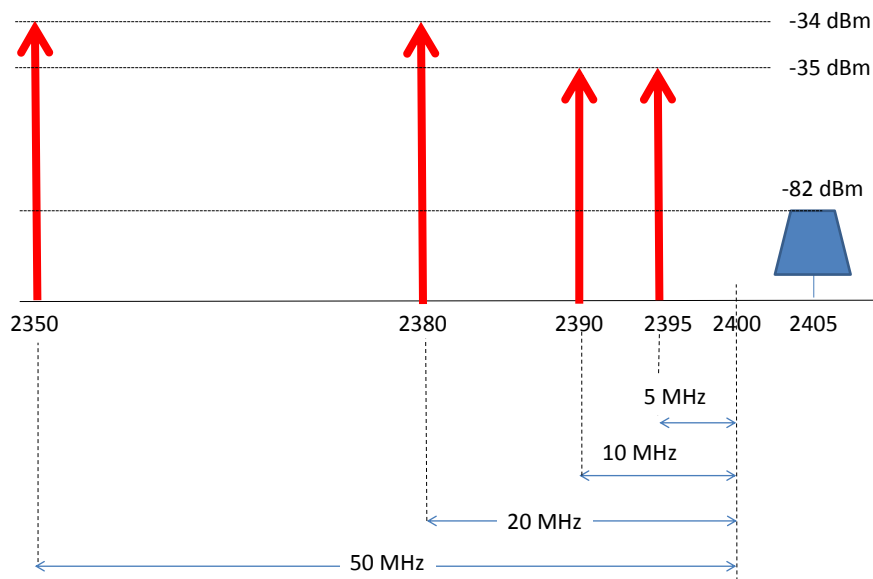
Figure 5   An illustration of CC2530 blocking performance.

This analysis is inconclusive in terms of determining whether the receiver performance of the ZigBee device or the TDD LTE OOBEs have the biggest impact on the performance of a ZigBee system and this issue was investigated further in the measurement programme. Note that a UE has been considered as the TDD LTE interferer in the analysis presented in this section. However, a BS would have a cleaner signal, resulting in lower levels of OOBEs. Also, the transmit power level and therefore, the MCL (and MSD) would be much higher compared to a UE. Our calculations for MCL and MSD in Section 9 have been performed for both UE and BS TDD LTE interferers.

5   Interference Mitigation Mechanisms

Once interference gets into the receive chain itself, the performance of the ZigBee device will be determined by the ability of the protocol stack to minimize the impact of the interference, provided that the receiver is not heavily blocked. Since ZigBee systems are designed to operate in unlicensed frequency bands where interference will appear and disappear without warning, various interference mitigation mechanisms have been built into the ZigBee protocol stack to address this issue and can be used by ZigBee equipment designers. Example mechanisms are as follows.

- Mechanisms at the IEEE 802.15.4 physical layer

  o The physical layer provides the capability to perform clear channel assessment (CCA) in its CSMA-CA mechanism. One of the CCA methods is energy detection (ED) over a certain threshold. The mechanism enables ZigBee devices to avoid channels experiencing high interference.

  o The physical layer is able to scan a set of channels provided by higher layers and provide scan results to allow higher layers to perform dynamic channel selection.

  o The quasi-orthogonal modulation scheme, whereby each symbol is represented by one of 16 nearly orthogonal pseudo-noise (PN) sequences enables low signal-to-noise ratio (SNR) and low signal-to-interference ratio (SIR) operation, typically in the region of 5 dB to 6 dB.

- The acknowledgement and retransmission capability of the IEEE 802.15.4 MAC layer improves the link quality.

- Mesh networking at the ZigBee NWK layer provides alternate routes from a source device to a destination device, potentially allowing packets to be routed around links that are particularly affected by interference.

- The acknowledgement and retransmission capability of the ZigBee APS layer increases end-to-end transmission reliability.

These interference mitigation mechanisms help to minimise the impact of interference, but their effectiveness varies depending on the quality of service requirements of the applications and the level and duration of interference. If interference is relatively low power and short in duration, the acknowledgement and retransmission mechanism can be effective. For relatively high levels of interference or long durations, the acknowledgement and retransmission mechanism may not be able to keep the link connected and a ZigBee node may be forced to perform a rescan and try to re-join the network or, even worse, form a new network on a different channel. This would cause service disruption to users. For example, when a user flicks a switch to turn on a light, nothing will happen or there will be a large delay.

Our review of ZigBee application profiles shows that some applications are designed to protect against service disruption by careful setting of protocol parameters. For example, in the ZigBee Home Automation profile, the number of network scan attempts is set to three and the time between scan attempts is set to one second. In the ZigBee Health Care Profile on the other hand, the number of network scan attempts is set to two and the time between scan attempts is set to 10 ms. This design is to ensure that a ZigBee device in a Health Care application can join a network more quickly. However, if interference persists, more scan attempts just mean more power consumption by the device.

Regardless of the ZigBee application, the key measure of the impact of TDD LTE interference to the ZigBee system is whether or not the service to the user is disrupted, which is determined by whether or not the interference can be rejected by the receiver and, if not, how effective the acknowledgement and retransmission mechanism are.

Based on this analysis, we will focus our measurements around a CW blocking test, a TDD LTE OOBE test and an acknowledgement/retransmission protocol test.

6 Testing Approach

In this section we present the methodology that was used to perform the tests on practical ZigBee equipment. We start by discussing our choice of ZigBee test devices and then go on to examine the manner in which the LTE interfering signal was created. We then describe the steps that were carried out for each of the different types of testing.

6.1 Selection of ZigBee Test Devices

In an ideal world, any testing would be performed on off-the-shelf ZigBee devices that are designed for specific practical applications, eg, smart meters, wireless lighting control systems. In general, the performance of such off-the-shelf wireless products is tested using packet loop back, whereby the device under test (DUT) is put into a special mode that causes it to send any received packets back to the source device. This allows any errors introduced on the wireless link to be measured at a test set without the need to provide any additional interfaces to the DUT. Unfortunately, the ZigBee standard does not mandate the support of a loop back test mode in ZigBee products. It may be that some products do support a test mode of this nature, but the risks associated with identifying a sufficient number of these products

and successfully gaining access to the test mode within the time constraints of this project meant that this was not a viable approach.

Instead, we have used development boards based on chipsets from a number of the major ZigBee chipset manufacturers as the DUTs in our measurement programme. By using development boards we have a degree of control over the behaviour of a DUT, whilst still allowing us to measure and compare the performance of different ZigBee chipsets. With this approach it is also possible to provide a wired RF connection to the DUT, instead of using a wireless connection via an antenna, and this leads to a more repeatable measurement set up. Appendix A provides the list of ZigBee devices that were chosen for our tests.

6.2   LTE Signal Characteristics

In testing of this nature it is important to use an interfering signal that is as representative of real TDD LTE equipment as possible. Previously Ofcom has commissioned measurements of OOBEs from LTE user equipment (UE) devices operating in the 800 MHz band [11]. A sample of these results is reproduced in Figure 6. It is noted that these devices include a band filter that will limit the OOBEs on the upper side of the occupied channel and, since this filter may not be present in equipment operating in the 2300 – 2400 MHz frequency band, it seems more appropriate to use the OOBEs on the lower side of the occupied channel as being representative of those associated with a UE in the 2300 – 2400 MHz band.
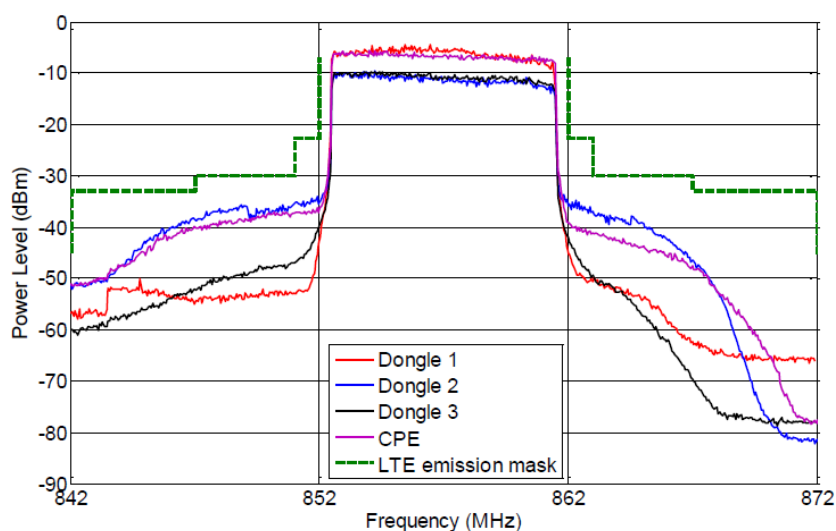
Figure 6   Measured LTE emissions from four UEs in the 800 MHz frequency band (10 kHz resolution bandwidth).

Ofcom has also provided MAC Ltd with some OOBE measurements for an LTE BS operating in the 2620 MHz to 2690 MHz frequency band using a channel bandwidth of 20 MHz. An example emissions plot for this BS is shown in Figure 7. MAC Ltd used the arbitrary waveform generation functionality and the associated signal libraries within the Rohde and Schwarz SMBV100A signal generator [12] to produce signals that are representative of the TDD LTE UEs and BSs for both a 10 MHz and 20 MHz carrier bandwidth. Figure 8 shows an example of the output from the SMBV100A that was used to represent a TDD LTE BS and this is compared with the European Telecommunications Standards Institute (ETSI) BS transmitter mask and the measurements provided by Ofcom. All of the resource blocks were used in our BS transmission signal.
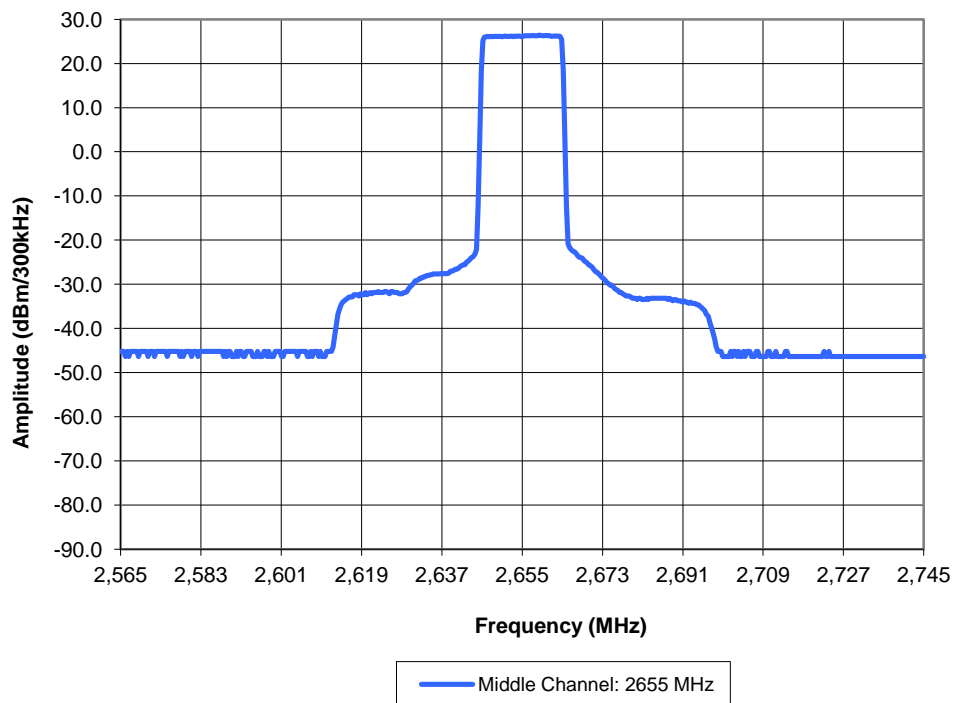
Figure 7   Example TDD LTE BS emissions measurement.
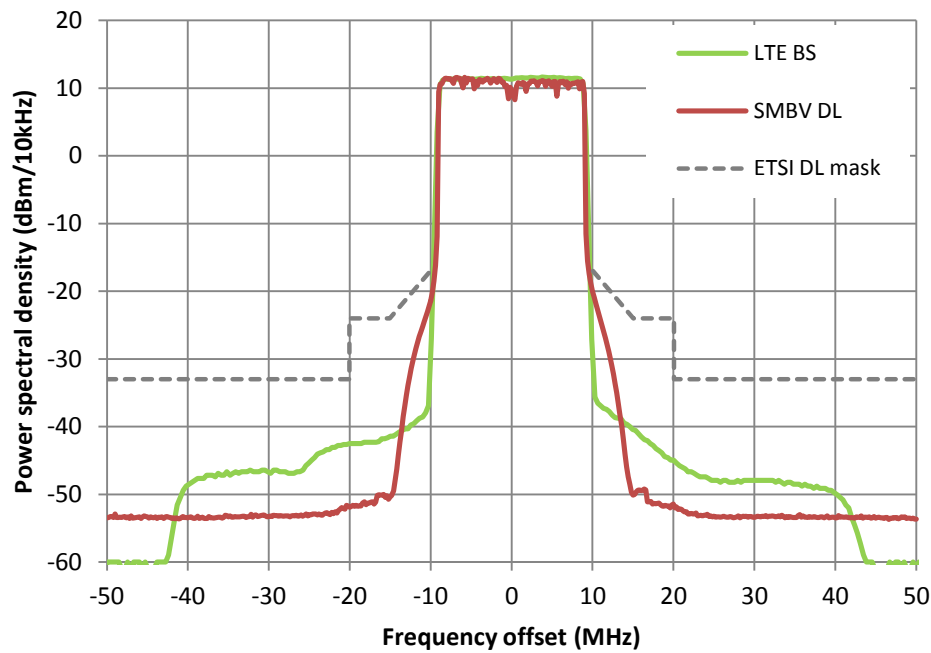
Figure 8   Representation of the TDD LTE BS transmission using the SMBV.

Figure 9 shows an example output from the SMBV representing the UE transmissions for a 10 MHz channel bandwidth and a comparison with one of the UE transmitter characteristics provided by Ofcom. The shows that the SMBV is able to match the UE transmitter characteristics closely, particularly on the lower side of the channel, which is the most relevant side for the reasons presented above. Again, all of the resource blocks were used in our UE transmission signal.

In addition to making the TDD LTE interfering signal as representative as possible, it is also important to match the time slot structure of the BS and UE transmissions. Table 1 shows the range of slot structures for the TDD LTE system. Configurations 0 and 5 (highlighted red in Table 1) represent the extreme cases of uplink-dominant and downlink-dominant transmissions, respectively. Configurations 1 and 3 (highlighted green in Table 1) are more balanced, but cover the two frame period options. In our testing we used Configuration 5 as the primary downlink configuration, with the downlink timeslots containing BS transmissions and inactive uplink timeslots. This configuration represents a relatively high transmission duty cycle (90%). Therefore, for the primary uplink configuration we used the more balanced Configuration 3 with the uplink timeslots containing UE transmissions and the downlink

timeslots inactive. In each case we used QPSK transmission as we do not believe that the chosen modulation scheme will have a significant impact on our test results.
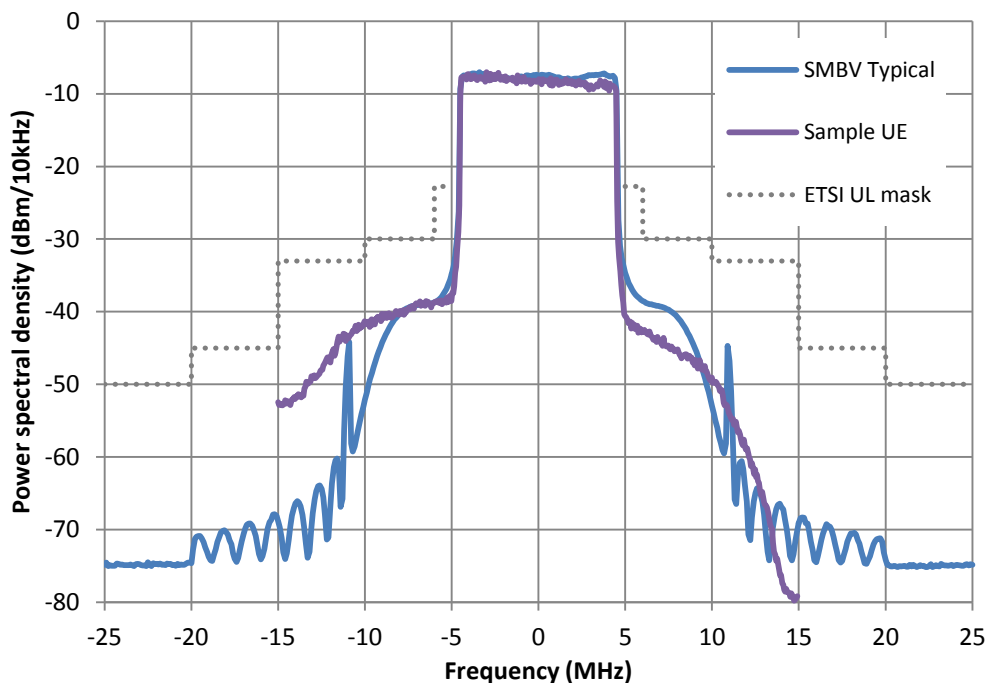
Figure 9   Representation of the TDD LTE UE transmission using the SMBV.

6.3 Test Programme

6.3.1 Test Set-up

The equipment arrangement used for the testing is shown below in Figure 10. The ZigBee test transmitter consists of a ZigBee development board and this was used to generate the 'wanted' ZigBee signals for testing. A digitally controlled variable attenuator was used to provide the fine control over the signal level produced by the ZigBee transmitter. As discussed above, the interfering LTE signal was simulated using a Rohde and Schwarz SMBV 100A vector signal generator and the wanted and interfering signals were brought together in a RF combiner. This combined signal was then fed, via a RF splitter, into the screened enclosure and connected to the device under test (DUT), which consisted of one of the ZigBee development boards. The other output from the RF splitter was used to monitor the combined signals on a spectrum analyser. For each of the development boards tested in this study, an identical development board was used as the ZigBee test transmitter.

Packet generation software was developed to run on the control PC and the development boards and this produced data that was sent from the ZigBee test transmitter to the DUT. The DUT was also connected to the control PC so that the packet error rate (PER) could be determined. In the following sections we examine each of the individual tests that were performed.
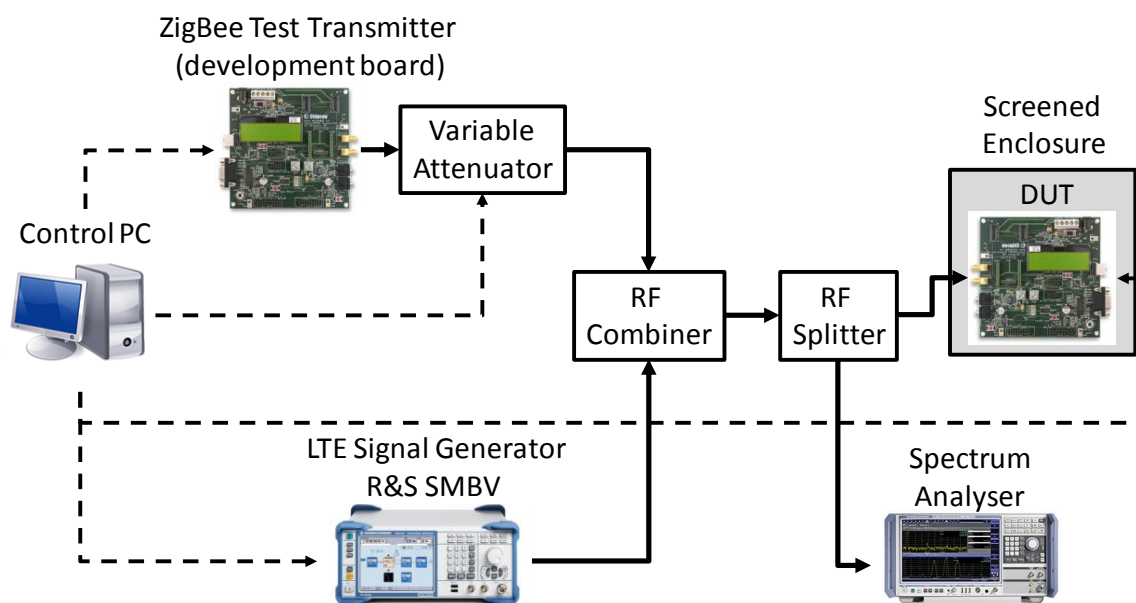
Figure 10　　Test Set-up (PC control connections shown with dotted lines, RF paths shown with solid lines.

6.3.2　LTE OOBE Test

For each DUT the test procedure to determine the carrier-to-interference protection ratio required to compensate for the presence of co-channel and adjacent channel TDD LTE transmissions was as follows.

1. With the LTE signal generator switched off and the power level from the ZigBee test transmitter set to a fixed value, the attenuation in the signal path was adjusted and the PER was measured to establish the reference sensitivity level for that DUT. The IEEE802.15.4 standards define the reference sensitivity based on a PER of <1% and after discussion with Ofcom it was agreed that this would be used as the reference 'minimum useable sensitivity' (MUS) in all of the tests. It should be noted, however, that the MUS associated with particular ZigBee applications and systems could be

significantly lower than this (ie, a significantly higher PER could be tolerated in particular scenarios).

2. The ZigBee transmitter was set to send packets periodically to the DUT on the lowest frequency ZigBee channel (Channel 11), at a power level of 10 or 20 dB above the MUS measured in (1).

3. The LTE signal generator was turned on and its power level was adjusted until the MUS PER was measured on the PC. The carrier-to-interference ratio (C/I) based on the output of the signal generator and ZigBee transmitter was recorded.

4. Steps (2) and (3) were repeated for each test configuration.

Ofcom defined the different test configurations to be investigated and it divided these into essential and non-essential tests. The essential tests are defined in Table 5 and these consist of measurements with the ZigBee test transmitter power set to 20 dB above the DUT's MUS. These tests were performed on each of the development boards (Devices 1 to 4) and also on the ZigBee USB stick (Device 5).

LTE Channel Bandwidth	ZigBee Receiver Sensitivity	Frequency Offsets	LTE Frame Structure	Measurement Combinations
20 MHz	+20 dB above MUS	Co-channel, 2380 MHz, 2360 MHz	UL and DL	6
10 MHz	+20 dB above MUS	Co-channel, 2385 MHz, 2375 MHz	UL and DL	6
Total Essential Tests per device				12

Table 5 Essential LTE OOBE Tests.

The non-essential tests are defined in Table 6 and they consist of measurements at 10 dB and 20 dB above MUS. These tests were only performed for Devices 1 and 2.

LTE Channel Bandwidth	ZigBee Receiver Sensitivity	Frequency Offsets	LTE Frame Structure	Measurement Combinations
20 MHz	+10 dB above MUS	2380 MHz and 2360 MHz	DL	2
10 MHz	+10 dB above MUS	2385 MHz and 2375 MHz	DL	2
10 MHz	+20 dB above MUS	2355 MHz and 2365 MHz	DL	2
Total Non-Essential Tests per device				6

Table 6 Non-Essential LTE OOBE Tests.

6.3.3 Receiver Blocking Test

In order to understand the selectivity and blocking performance of a ZigBee receiver, tests were also performed using a carrier wave (CW) signal as the interfering signal. The following process was used to perform these measurements. The LTE transmitter in Figure 10 was configured to transmit a simple CW signal.

1. The MUS of the ZigBee DUT was determined using Step 1 from the OOBE tests above.

2. The variable attenuator was adjusted to increase the signal from the ZigBee transmitter by a selected amount (eg, 20 dB).

3. The CW power was then increased gradually until the MUS performance was reached (ie, PER < 1%). The transmitted power of the CW transmitter was recorded.

4. Step 3 was repeated for different transmit frequency settings of the CW transmitter. An initial frequency step size of 5 MHz was used, but a smaller step size of 1 MHz was used close to the ZigBee channel to provide a higher resolution.

The receiver blocking tests have also been divided into essential and non-essential tests. The essential tests were performed on all the ZigBee devices selected for this study. In agreement with Ofcom, the non-essential tests were only performed on Devices 1 and 2. These tests are defined in Table 7.

ZigBee Receiver Sensitivity	Number of Devices	Comments
+20 dB above MUS	5	Essential
+10 dB above MUS	2	Non-Essential

Table 7 Receiver Blocking Tests.

6.3.4 Acknowledgement and Retransmission Protocol Test

In addition to the lower layer performance testing of different ZigBee devices, Ofcom is also interested in the impact of the features provided by the higher layers in the protocol stack on the ZigBee link performance and its resilience to TDD LTE interference. Therefore PER and throughput measurements were collected for one of the developments boards for a received signal level close to the MUS and without any interference and for a received signal level of

20 dB above the MUS in the presence of different levels of TDD LTE interference with packet acknowledgements and retransmissions enabled.

6.3.5 Application-specific ZigBee Testing

The final tests performed as part of this study were designed to understand the impact of TDD LTE interference on an off-the-shelf ZigBee system deployment in a manner that represents a real-world application. To this end, a home automation system based on the ZigBee technology was procured and a simple lighting control system was deployed in MAC Ltd's office. This consisted of placing the main home automation control unit at one end of the office and the ZigBee-enabled mains relay (which controls the light) and a ZigBee-enabled in-room remote control switch at the opposite end of the office. The separation of the main control unit from the relay and remote control was about 32 m. The remote operation of the relay, which requires a link from the remote control unit to the main control unit and from the main control unit back to the relay, was tested both with and without TDD LTE interference and any performance impact of the interference was noted.

7 Test Results

The results of the LTE OOBE and CW blocking tests performed on the selected ZigBee devices are presented in this section. The procedure used for calibrating the test set-up is described in Section 7.1. The results obtained from these tests are presented in Section 7.2. The essential tests (see Table 5 and Table 7) were performed on five different devices (Devices 1 to 5) based on chipsets from four different vendors (Vendors 1 to 4). The non-essential tests (see Table 6 and Table 7) were performed on devices based on chipsets from only two vendors (Vendors 1 and 2).

Note that the results of acknowledgment and retransmission protocol tests and ZigBee application tests have been presented later in separate sections and are not discussed here.

7.1 System Calibration

Figure 11 shows a simplified block diagram of the test system illustrated in Figure 10. The test system was calibrated to ensure the accurate recording of the wanted and interference signal strengths delivered to the device under test (DUT) during the testing. This included the following steps:

- Measuring the actual transmit power levels of each of the devices that were used to generate the wanted ZigBee signals.

- Measuring the actual attenuator values provided by the digital variable attenuator at each setting.

- Measuring the loss in the ZigBee signal path (from the ZigBee transmitter to the RF input port on the DUT).

- Measuring the loss in the interference path (from the signal generator to the RF input port on the DUT).

These steps are discussed in the following sections.
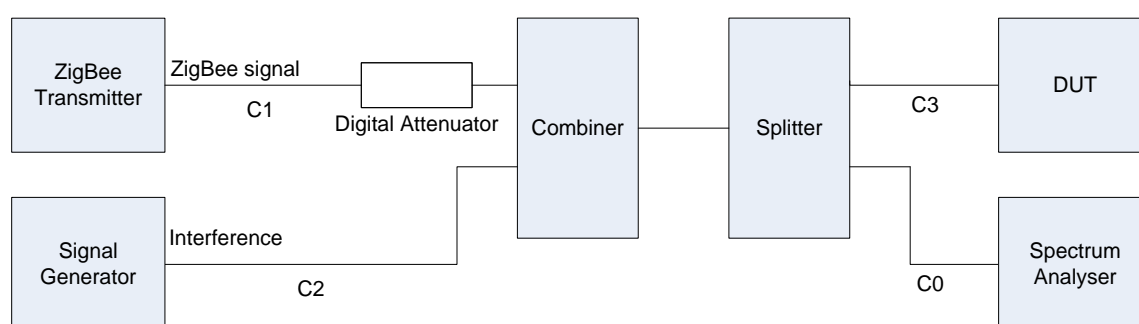
Figure 11   Block diagram of the test system used for performing the interference measurements.

7.1.1 Measurement of ZigBee Transmit Power Levels

As previously mentioned (in Section 6.3.1), each ZigBee development board (DUT) was tested using an identical development board as the transmitter. Therefore, the transmit power levels were different for each development board due to different options being made available by their respective vendors in the test software. The transmit power levels were measured by connecting the development board directly to a spectrum analyser via an RF cable (C0). This cable, in turn, was also calibrated by using it to connect a signal generator to a spectrum analyser. The loss for this cable was measured by passing a CW signal through it and recording the difference between the transmitted and received power levels. The next step was to measure the power received at the spectrum analyser when a wanted ZigBee signal was transmitted by each of the development boards. The centre frequency of the spectrum analyser was set to ZigBee Channel 11 (2405 MHz) and the channel power was measured by capturing the maximum power within a 2 MHz bandwidth around the centre frequency across a number of snapshots. It was necessary to use this 'peak hold' approach

because a number of the devices used could only transmit in discontinuous packet mode, rather than a continuous mode, and this made it difficult to measure a meaningful average transmitted power.

Table 8 shows a comparison between the transmit power levels measured in our calibration process and the nominal transmit power settings for the ZigBee devices. Note that Table 8 does not show the transmit power level for Device 5, because Device 4 was used as the transmitter during the interference testing of Device 5.

Device	Transmit Power Level (dBm)	
	Measured	Nominal
Device 1	-17.1	-17
Device 2	-3.3	-4
Device 3	-11.1	-11
Device 4	1.3	3

Table 8 Calibration results for the transmit power levels for the ZigBee devices.

The nominal transmit powers shown in Table 8 do not represent the maximum transmit powers of these devices; instead they are the power level settings that we have chosen to use in our tests. The chipsets tested in this study all offer maximum transmit power levels that are similar to each other (ie, they are within 1 dB of each other) although some companies offer ZigBee modules capable of higher transmit output powers for longer range applications.

7.1.2 Digital Attenuator

The different levels of the wanted (ZigBee) signal were generated by placing a variable attenuator in the signal path and controlling its attenuation digitally using a MATLAB control script. We used the Lab Brick™ digital attenuator (Model: LDA-602), manufactured by Vaunix Technology Corporation [13] for this purpose. This attenuator can provide an attenuation from 0 to 63 dB in 0.5 dB steps. Before running the sensitivity and interference tests, we calibrated the digital attenuator by placing it between our signal generator and spectrum analyser. The attenuator was initially set to 0 dB and the total path loss was measured. Next, the attenuation was increased in steps of 0.5 dB and the increase in path loss was recorded. A total of 100 measurements were recorded and averaged for each attenuator setting (including 0 dB). These results were taken into account when calculating the receiver sensitivity and C/I values for CW blocking and LTE OOBE tests.

7.1.3 Loss in ZigBee and Interference Paths

The last step in the calibration process was to measure the attenuation suffered by the ZigBee and interfering signals before they reach the input of the DUT. The loss for the wanted ZigBee signal was measured by replacing the ZigBee transmitter with the signal generator and replacing the DUT with the spectrum analyser and transmitting a CW signal through the ZigBee signal path. Similarly, the loss for the interfering signal was measured by transmitting a CW signal through the interference signal path using the signal generator and measuring the power received on the spectrum analyser. The results obtained from these measurements were used in our final calculations.

7.2 Measurement Results

The test results for each of the devices are presented in this section. For ease of reference, the following conventions are used for plotting the graphs presented in this section.

- Colour indicates the interferer type
  - —— green indicates 10 MHz TDD LTE downlink interferer
  - —— blue indicates 10 MHz TDD LTE uplink interferer
  - —— purple indicates 20 MHz TDD LTE downlink interferer
  - —— orange indicates 20 MHz TDD LTE uplink interferer
  - —— brown indicates CW interferer
- For LTE interferers, markers are used for indicating the uplift level (ie, the margin above minimum useable sensitivity).
  - —•— dot indicates 20 dB uplift
  - —□— Square indicates 10 dB uplift

When the results for different devices are being compared on the same plot, then colours are used to differentiate between the devices and this will be explained in the legend inside the figure. Frequency markers in the form of vertical dashed lines indicate the centre frequency of the proposed LTE channels closest to the 2.4 GHz band. These channels are located at 2385 MHz for 10 MHz LTE and at 2380 MHz for 20 MHz LTE signals. In terms of frequency offset relative to a ZigBee channel at 2405 MHz, these channels are located at -20 and -25 MHz respectively. The vertical lines are colour coded when both 10 MHz (green) and 20 MHz (purple) LTE interferers are shown in a figure.

In addition to the essential test points specified by Ofcom (Table 5 and Table 7), the tests were also performed at other frequency offsets for Devices 1 and 2 in order to gain a better understanding of the behaviour of these devices. These additional test points were not measured for Devices 3, 4 and 5.

In the following sections, the term 'target C/I' refers to the minimum C/I ratio needed to achieve a PER of less than 1%, and 'interference tests' refers to CW blocking and LTE OOBE tests.

7.2.1   Device 1

Figure 12 shows the results of the essential interference tests for Device 1. The *x*-axis shows the frequency difference between the centre frequency of the interferer and the wanted ZigBee signal (ie, 2405 MHz) and the *y*-axis shows the target C/I for a 1% PER. The results are plotted for 10 MHz and 20 MHz LTE interferers in both the uplink and downlink directions. In order to compare the 10 MHz and 20 MHz plots it is necessary to 'slide' the 20 MHz plot 5 MHz to the right to align the upper edges of the TDD LTE channels.

LTE Frame Configuration 5 with a BS spectrum (see Figure 8) was used to represent the downlink and Frame Configuration 3 with a UE spectrum (see Figure 9) was used to represent the uplink. Note that the curves are based on more data points than specified by Ofcom as part of its essential tests (see Table 5). The additional data points were measured to gain a better understanding of the behaviour of this device. The ZigBee signal was 20 dB above the MUS of the receiver. The MUS for Device 1 was measured prior to running the interference tests and it was found to be -92.1 dBm. Therefore, the ZigBee signal strength at the RF input of the DUT was -72.1 dBm.

The CW blocking test results show that the target C/I for a co-channel CW interferer is 8 dB. In comparison, the target C/I for co-channel LTE interference is approximately 2.5 dB for a 10 MHz TDD LTE interferer and -0.5 dB for a 20 MHz TDD LTE interferer. This decrease in the co-channel target C/I is to be expected as the bandwidth of the interfering signal increases beyond the nominal ZigBee receiver bandwidth of 2 MHz. The CW blocking plot appears to show the side lobes of the receiver filter.
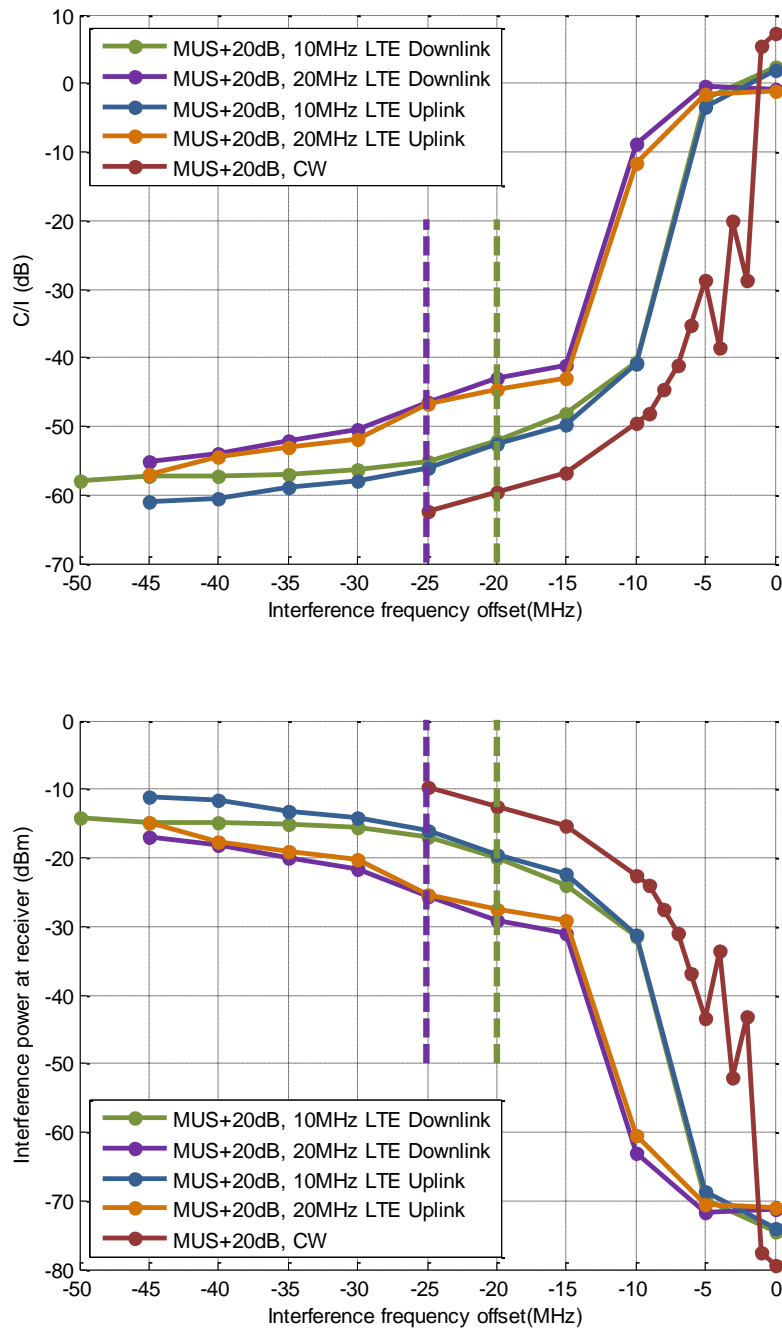
Figure 12   Essential interference test results for Device 1 showing the performance in the presence of UL and DL TDD LTE interference, with 20 dB uplift above MUS. The MUS for Device 1 was measured to be -92.1 dBm.

A comparison of the target C/I values with two different levels of uplift are shown in Figure 13. Three sets of results are presented; CW blocking measurements and OOBE measurements for 10MHz downlink and 20 MHz downlink TDD LTE interferers. Each type of test was run with the ZigBee signal at 20 dB and 10 dB above the MUS. The CW curve

with 10 dB uplift was generated at a lower resolution compared to the 20 dB uplift case, and therefore, the points on this graph have not been joined with a line.
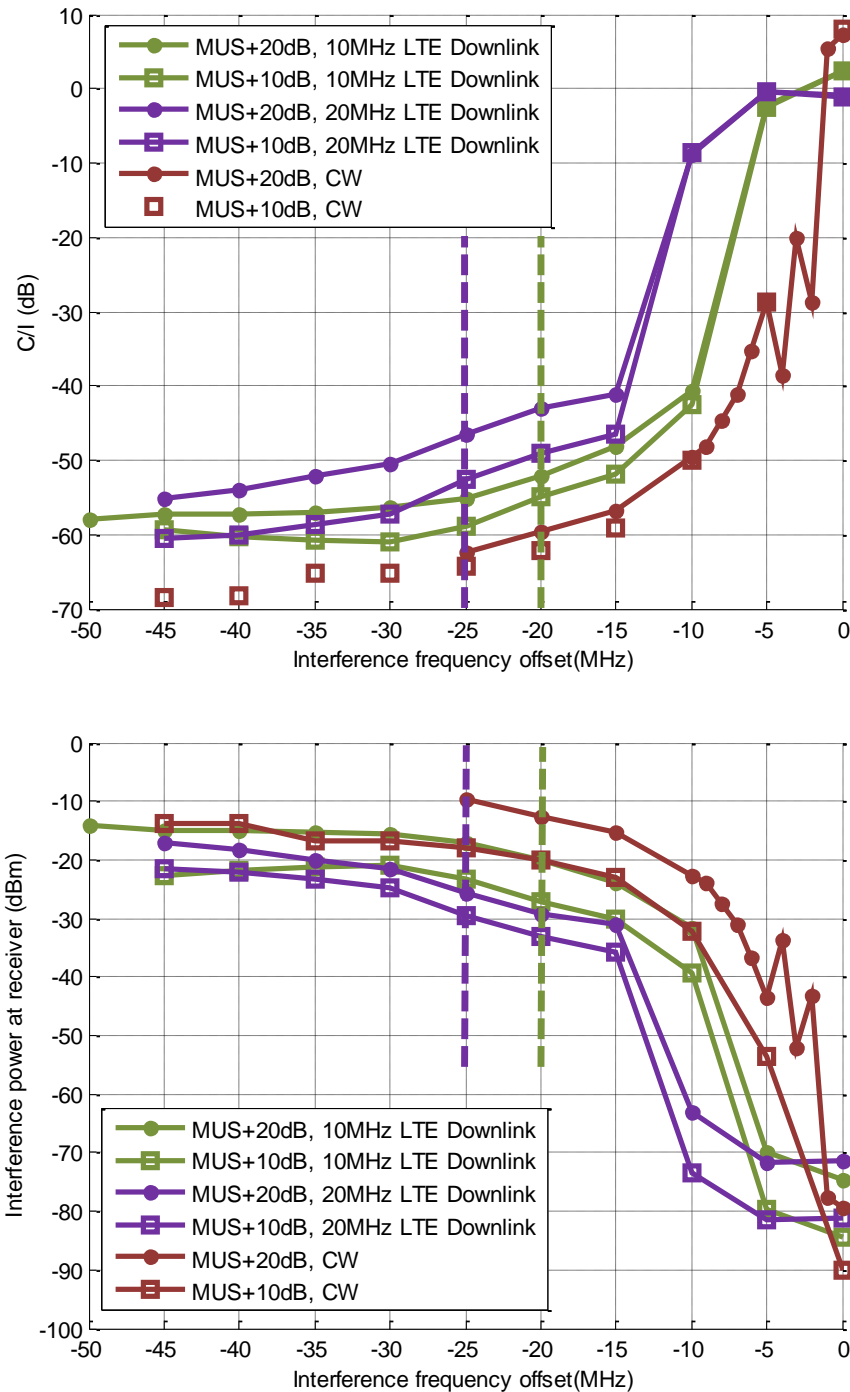
Figure 13   Comparison of interference test results for Device 1 with 20 dB and 10 dB uplift above MUS. (MUS = - 92.1 dBm).

7.2.2 Device 2

The results of the essential interference tests for Device 2 are presented in Figure 14. The MUS of this device was measured to be -95.3 dBm. At an uplift of 20 dB, the device exhibits a target C/I of 0.8 dB for a co-channel CW interferer, and -1.5 and -4.8 dB for 10 MHz and 20 MHz TDD LTE interferers, respectively. The C/I curves for LTE OOBE tests converge towards a floor value of approximately -53 dB for frequency offsets of -30 MHz and beyond. The curves for the 10 MHz and 20 MHz TDD LTE interferers reach the floor value at approximately -20 MHz and -30 MHz offsets, respectively.
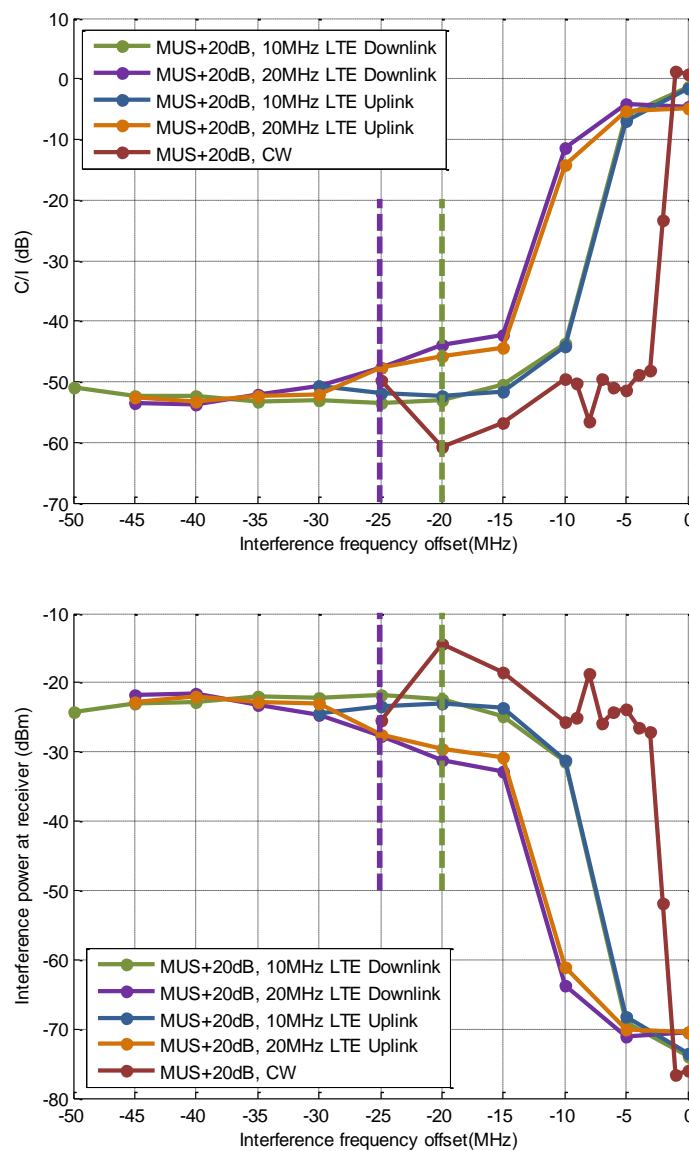
Figure 14   Essential interference test results for Device 2. The MUS
for Device 2 was measured to be -95.3 dBm.

A comparison of perform of Device 2 with different uplift levels is shown in Figure 15.
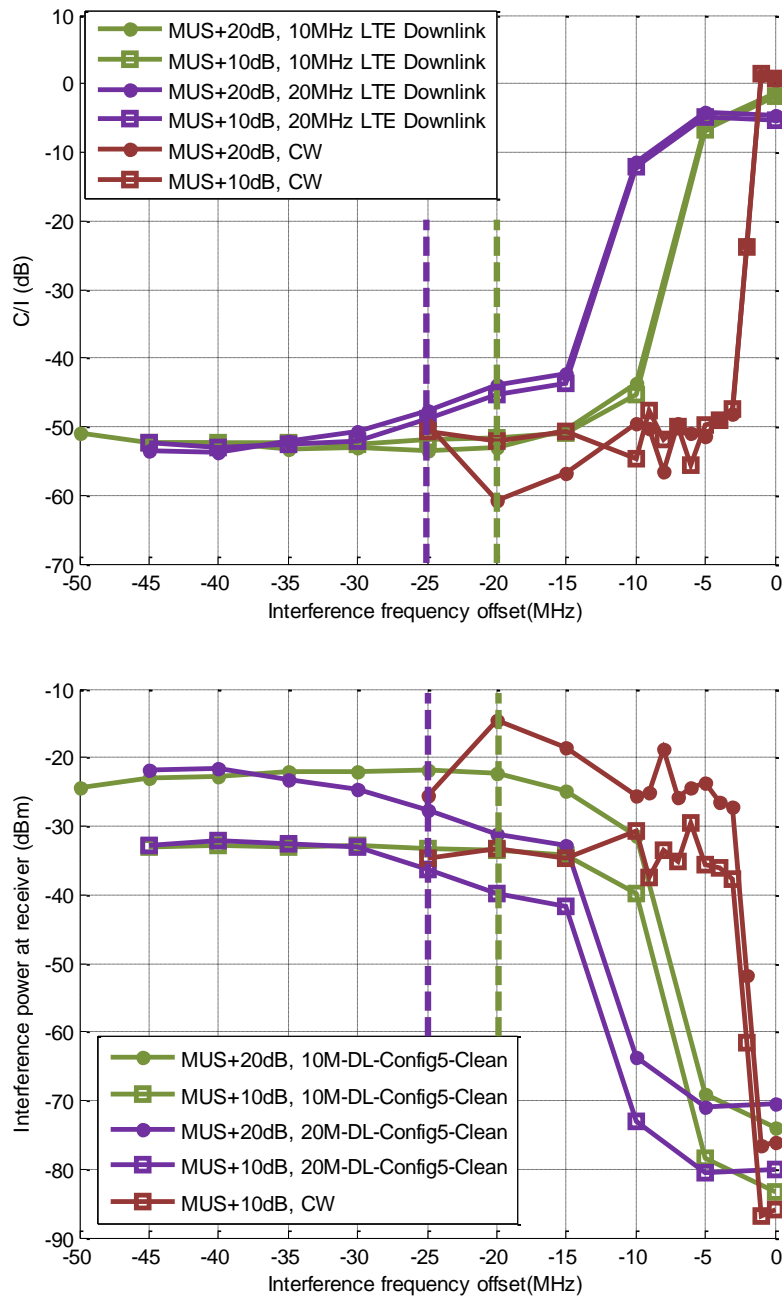
Figure 15   Comparison of interference test results for Device 2 with 20 dB and 10 dB uplift above MUS. (MUS = -95.3 dBm).

7.2.3   Device 3

The results for the LTE OOBE and CW blocking tests for Device 3 are presented in Figure 16 for MUS+20 dB. The MUS of this device was measured to be -90.8 dBm. The target C/I for a co-channel interferer is 4.9 dB for a CW interferer, and approximately -0.3 and -3.5 dB for 10 MHz and 20 MHz TDD LTE interferers, respectively. At large frequency offsets, the floor value of target C/I is approximately -57 dB for the 20 MHz interferers and this value occurs at an offset of -45 MHz. The target C/I graph for the 10 MHz interferers also reaches this floor value at a frequency offset of -20 MHz. However, at a frequency offset of 30 MHz, the target C/I for the uplink interferer is slightly higher compared to the downlink interferer.
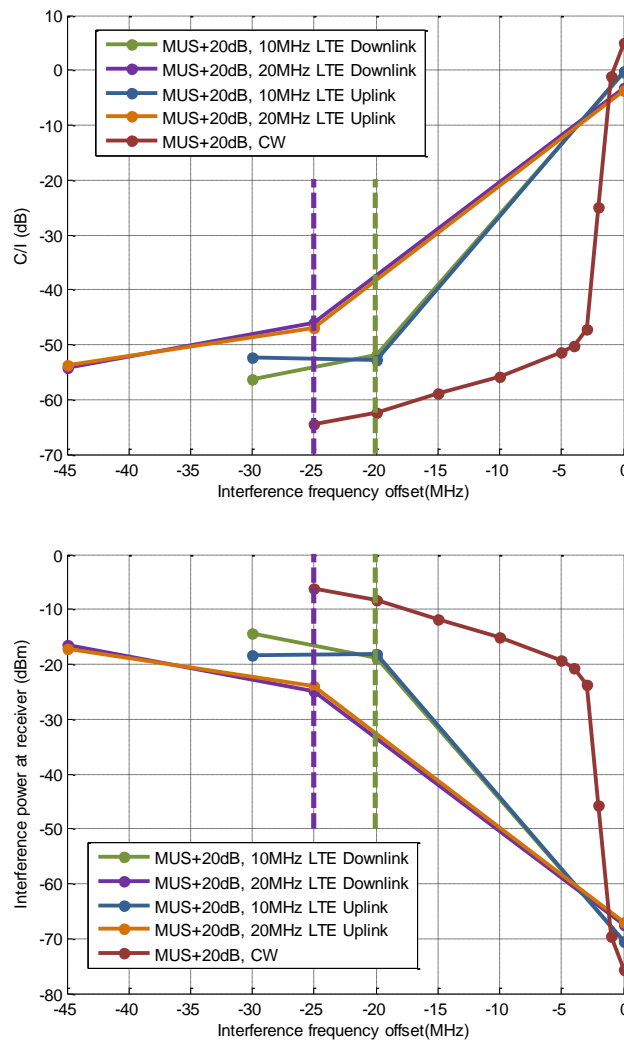
Figure 16   LTE OOBE and CW blocking test results for Device 3.
(MUS = -90.8 dBm).

7.2.4 Device 4

The results for the LTE OOBE and CW blocking tests for Device 4 are shown in Figure 17 for MUS+20dB. The MUS for this device was found to be -99.7 dBm. The target C/I for a co-channel interferer is 6.3 dB for a CW interferer, and approximately -2.6 dB and -5.8 dB for 10 MHz and 20 MHz TDD LTE interferers, respectively. The target C/I curve for the CW interferer reaches a floor of approximately -58 dB. The shape of the target C/I curves for the LTE interferes also suggest that they would reach this floor, however, this could not be verified over the range of frequency offsets for which this test was performed.
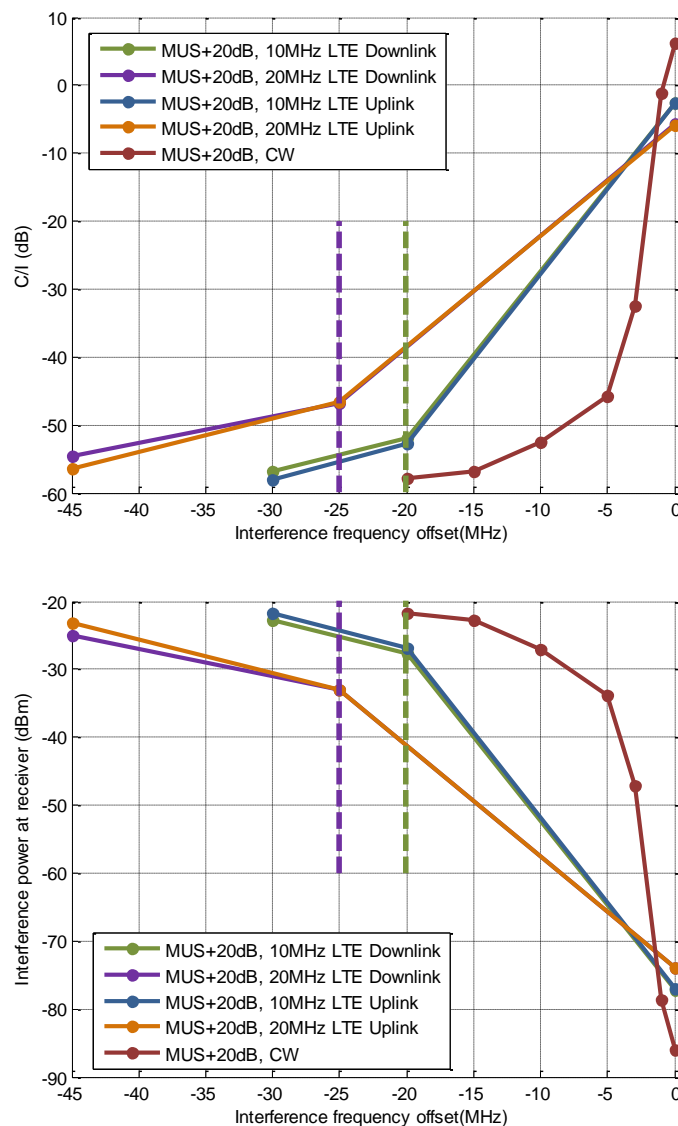
Figure 17   LTE OOBE and CW blocking test results for Device 4.
(MUS = -99.7 dBm).

7.2.5   Device 5

The test set-up for Device 5 was slightly different compared to the other devices tested during this study. Device 5 is based on the same chipset as the one used in Device 4. However, this device has the physical form of a USB stick with an on-board integrated antenna. Therefore, we modified the test set-up by placing an antenna inside the screened enclosure to communicate with the DUT wirelessly over a short air gap. The results for the LTE OOBE and CW blocking tests for Device 5 are shown in Figure 18. Note that the test did not complete for 10 MHz TDD LTE uplink interferer at 2360 MHz (45 MHz offset) due to insufficient maximum allowed power in the signal generator.
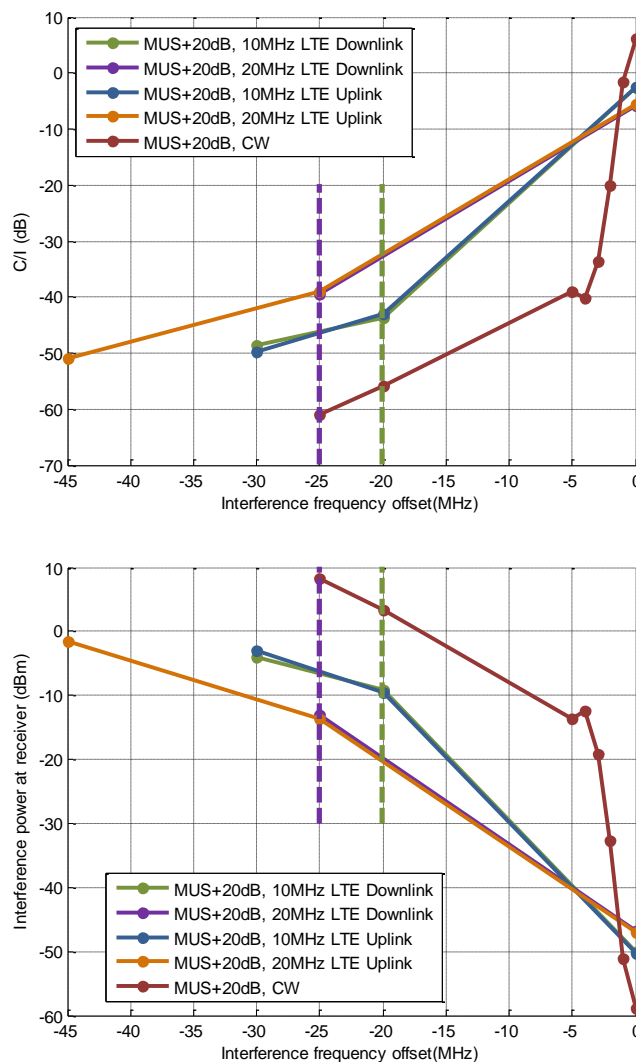
Figure 18   LTE OOBE and CW blocking test results for Device 5. The MUS for Device 5 could not be measured due to the presence of air gap in the signal path.

8   Analysis

8.1   Minimum Useable Sensitivity

A comparison between the nominal reported receiver sensitivity for the chipsets tested in this study and the MUS values measured in our tests is shown in Table 9. The measured values of receiver sensitivity for Device 2 and 4 match reasonably well with their nominal chipset values. However, the discrepancy between these values is approximately 9 dB for Device 1 and 4.2 dB for Device 3.

Note that the MUS for Device 5 has not been listed in Table 9. This is because this device has an on board integrated antenna, and therefore, the input RF cable was connected to an antenna (inside the screened enclosure). The presence of this wireless link added an unknown amount of attenuation in the link. Therefore, it was not possible to determine accurately the signal strength at the RF input of Device 5.

Device	Receiver Sensitivity (dBm)	
	Nominal	Measured
Device 1	-101	-92.1
Device 2	-98	-95.3
Device 3	-95	-90.8
Device 4	-100	-99.7

Table 9   Comparison between the nominal and measured values
of receiver sensitivity for the devices tested in this study.

8.2   Sensitivity to TDD LTE and CW Interference

In this section we discuss the effects of TDD LTE and CW interference on the performance of the ZigBee devices using the results for Device 1 and 2 as examples. The general trend observed from this study is that while the frequency offset between the centre frequencies of the ZigBee and TDD LTE channels is less than 5 MHz, the main lobe of the 20 MHz interferer fully covers the ZigBee channel, and therefore, the target C/I ratio remains unchanged. On the other hand, the target C/I begins to reduce for the 10 MHz interferer for offsets of just 5 MHz, as the main lobe of the interferer does not fully cover the ZigBee channel. This can be clearly observed from Figure 12 (Device 1) and Figure 14 (Device 2). We believe that similar behaviour would be exhibited by Devices 3, 4 and 5, although we do not see this in our results due to the lower resolution of the collected data points.

As the frequency offset between the ZigBee signal and the LTE interferers is increased, the edge of the TDD LTE transmission signal moves away from the ZigBee channel, and the interference power needed to degrade the PER below 1% increases sharply, causing the target C/I to drop. At large frequency offsets between the ZigBee and LTE signals, the target C/I tends towards a 'floor' value. However, the target C/I curve for the 10 MHz TDD LTE interferer converges towards the floor value much faster compared to the 20 MHz TDD LTE interferer. A possible explanation could be the spectral shape of the LTE signal generated by the SMBV100A signal generator ('SMBV'). The signal spectrum in Figure 8 is an example of a 20 MHz TDD LTE signal used as the downlink interferer in this study. It can be observed that this signal reaches its floor value at an offset of about 25 MHz relative to its centre frequency. Also, the 10 MHz TDD LTE spectrum generated by the signal generator (not shown in Figure 8) reaches its floor value at an offset of about 15 MHz. Therefore, it is to be expected that the target C/I curve for 20 MHz LTE interferer would reach its floor at a much larger frequency offset than a 10 MHz LTE interferer. However, other interference mechanisms may also be observed as discussed next.

For example, it can be observed from Figure 13 (Device 1) that an increase of about 3 to 4 dB in power level of the 20 MHz LTE interferer is enough to 'cancel out' (ie, bring the PER back up to around 1%) a 10 dB increase in the ZigBee signal level. This behaviour is observed at frequency offsets of -15 MHz and beyond. This is consistent with the behaviour expected when third-order intermodulation products are being generated due to the non-linear behaviour of the receive chain. Since the received power levels increase dramatically at frequency offsets of -15 MHz and larger, we can expect that the receiver has been driven into its non-linear region. A similar effect can be observed by comparing the curves for the 10 MHz TDD LTE interferer at 10 and 20 dB above MUS. The difference between these two graphs is between 6 and 7 dB, suggesting that although the receiver is showing non-linear behaviour, third-order intermodulation is less dominant for the 10 MHz TDD LTE interferer.

.In contrast, Device 2 does not display evidence of the presence of intermodulation products. Figure 15 shows the interference power at the receiver input of Device 2 for CW and TDD LTE (20 and 10 MHz) interferers. It can be seen that a 10 dB increase in the LTE signal level is needed to counter (ie, bring the PER back up to 1%) a 10 dB increase in the ZigBee signal level. Therefore, we conclude that Device 2 is not being driven into its non-linear region at these interference levels.

Another important difference between Device 1 and 2 is revealed by comparing their response to CW and LTE interference. For example, with a 20 dB uplift above MUS in the ZigBee signal level, Device 1 can tolerate a CW interference level approximately 10 dB higher compared to the LTE interference levels (both 10 and 20 MHz) at large frequency offsets (such as -45 MHz). Consequently, the target C/I curve for CW has a much lower floor compared to the LTE interferers (see Figure 13). In contrast, Device 2 can tolerate the same power levels of CW and LTE interferers at large frequency offsets (for the same levels of ZigBee signal uplift). As a result, the target C/I floor levels in Figure 15 are the same for CW and LTE interferers. This suggests that the receiver is being desensitised (or blocked) due to high levels of interference entering the receive chain irrespective of the spectral shape of the interferer. Therefore, we can conclude that neither intermodulation nor OOBE from the LTE interferers are the dominant interference mechanisms for Device 2 at large frequency offsets. In the absence of a detailed knowledge about the actual receiver implementation, we cannot be certain about the exact mechanism that is causing the desensitisation of Device 2. It is possible that the automatic gain control (AGC) in this device responds to high levels of interference and reduces the gain of the front-end amplifier, thereby desensitising the receiver, but preventing it from being driven into its non-linear region.

Therefore, our analysis for Device 1 and 2 can be summarised as follows:

- Device 1 showed evidence of the presence of intermodulation products, suggesting that the receiver was being driven into non-linear operation due to high levels of interference. No evidence of non-linear behaviour was found for Device 2.
- For Device 2, the floor level of the target C/I curves for the LTE interferers is the same as that for CW. This suggests that the dominant interference mechanism in Device 2 is the desensitisation of the receiver due to the levels of interference power entering the receive chain, irrespective of the spectral shape of the interferer. In contrast, Device 1 is affected more strongly by LTE interferers compared to CW interferers, which is likely to be due to intermodulation products generated by the LTE interference.

Comparing the target C/I floor levels for CW and LTE signals, we find that the behaviour of Device 3 (see Figure 16) is similar to that of Device 1 in the sense that the CW signal has a much lower floor level compared to the LTE signal. For Device 4 (see Figure 17), the target C/I floor level for the CW and LTE interferers appears to be the same. This behaviour is

similar to that of Device 2. We cannot reach any conclusions regarding the presence of intermodulation products for Devices 3 − 5 as these devices were tested only at a single level of ZigBee signal (20 dB above MUS).

Next, we compare the behaviour of Device 1 and 2 with the rest of the ZigBee devices (ie, Devices 3, 4 and 5) in the presence of TDD LTE interferers. Figure 19 compares the performance of Devices 1 - 5 in the presence of a 20MHz and 10 MHz TDD LTE downlink interferer, with the ZigBee signal 20 dB higher than the MUS. The tests were performed only at essential frequencies for Devices 3 to 5, and the results for these devices have a much lower resolution. Therefore, the data points for these devices have not been joined together in this (and subsequent) plots.

It can be seen that all the devices, except Device 5, show very similar behaviour at the test frequencies. The results for Device 5 are similar to other devices for co-channel interferers. However, the target C/I appears to be much higher at 20, 25 and 30 MHz offsets. A possible reason is that the frequency response of the combined transmit and receive antennas used in this set up is not flat, and the path loss at these frequency offsets is less than that on the ZigBee channel. The results for Device 5 are inconclusive as to whether its behaviour is dominated by OOBE or blocking. We expected its behaviour to be similar to Device 4 as both devices are based on the same chipset. However, the results in Figure 18 show that the target C/I floor level for the CW interferer is much lower compared to the LTE interferers.
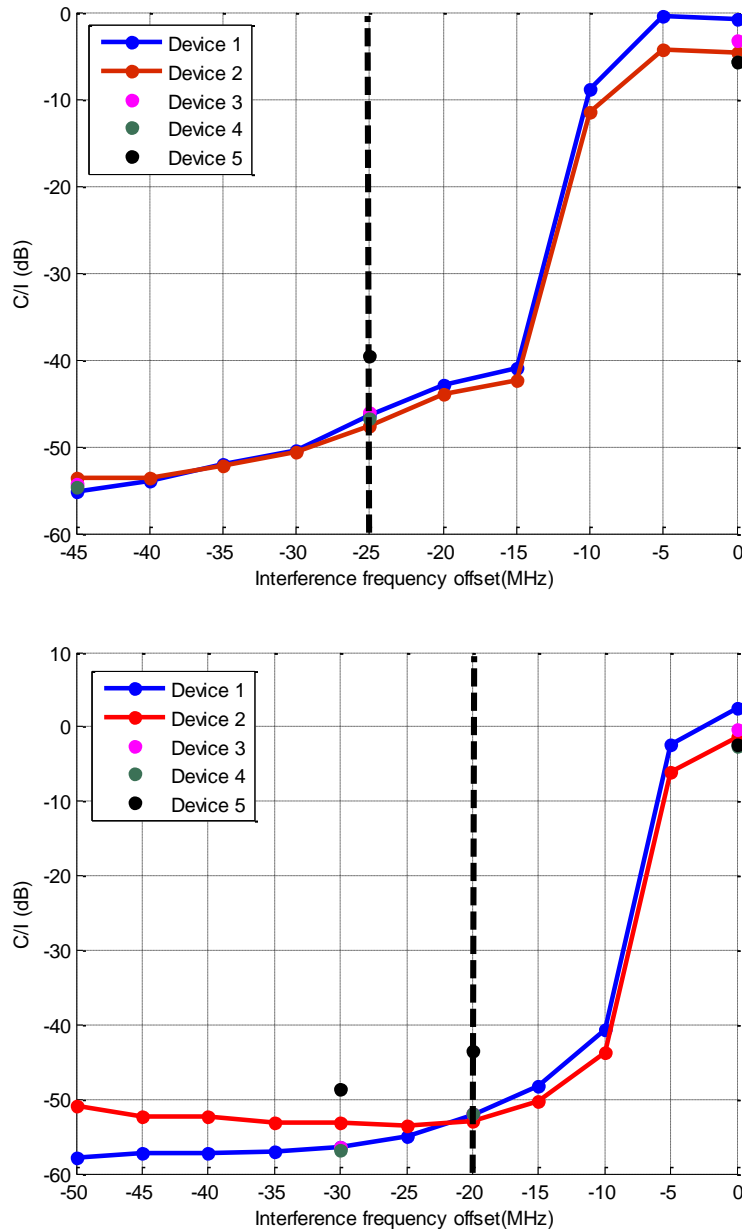
Figure 19   Test results, with ZigBee signal at MUS+20 dB, in the presence of (upper) 20 MHz TDD LTE downlink interferer and (lower) 10 MHz TDD LTE downlink interferer.

8.3   Downlink *vs* Uplink LTE Transmission

The plots showing the results of essential OOBE tests (Figure 12, Figure 14, Figure 16, Figure 17 and Figure 18) provide a comparison between the effects of uplink and downlink LTE interferers. It can be seen that the two sets of curves (ie, downlink and uplink) closely track each other. We might have expected the ZigBee link to perform better in the presence of uplink interference because the downlink transmissions use Frame Configuration 5, which

involves a relatively high transmission duty cycle (as described in Section 6.2), compared to the uplink, in which Frame Configuration 3, which has a lower transmission duty cycle, is used. Therefore, the probability of a ZigBee packet not being received by the DUT would be higher in the presence of a downlink LTE interferer, resulting in a slightly poorer performance at the reference sensitivity. However, this duty cycle effect may be compensated to some extent by the fact that the typical spectrum used for uplink transmissions has a wider skirt, as shown in Figure 9.

9 Minimum Coupling Loss and Separation Distance Analysis

In this section we examine the minimum coupling loss (MCL) and minimum separation distance (MSD) that is required between a ZigBee device and a TDD LTE interferer to limit the degradation at the ZigBee device using the target C/I values reported in the previous section. The MCL and MSD have been calculated for a worst case scenario of the ZigBee device operating at the lower end of the ISM band (ie, Channel 11, 2405 MHz) and the TDD LTE interferer occupying the upper end of the release band (ie, a centre frequency of 2385 MHz for a 10 MHz TDD LTE interferer and 2380 MHz for a 20 MHz TDD LTE interferer). The calculations were performed both for a UE and a BS as the source of interference. The TDD LTE UE has a maximum transmit power of 23 dBm [10] and an antenna gain of 0 dBi will be assumed. For a TDD LTE BS, a maximum transmit power of 64 dBm and 67 dBm will be assumed for 10 MHz and 20 MHz LTE signals, respectively, taking into account typical BS antenna gains.

Turning to the characteristics of the practical ZigBee device, the development boards used in our measurements were chosen because they have RF connectors that allow conductive tests to be performed, which are easier to control than tests using radiated signals. However, practical application-specific ZigBee devices are likely to use integrated antennas to allow the size of the device to be decreased to a minimum. Therefore, in order to interpret the practical implications of the measurement results collected during this project, it is important to understand the likely performance of the antennas used in ZigBee devices. Examples of antennas being used in ZigBee devices include the antennas supplied by Antenova (Rufa 2.4 GHz SMD Antenna Part No. A5839 [14]) and they have a peak gain of 2.1dBi and an average gain of -1.2dBi. Linx Technologies also provide ceramic chip antennas for use in ZigBee devices (ANT-2.45-CHP-B [15]) and these have a maximum gain of 0.5 dBi. A multilayer chip antenna provided by Rainsun (AN1003 [16]) could also be used in ZigBee

products and these have a peak gain of 1dBi. Therefore, for the purposes of determining the MCL and MSD between ZigBee devices and interfering TDD LTE devices, it would appear that a representative peak antenna gain for the ZigBee device is 2.1 dBi.

In order to convert a MCL value into a MSD value, we used a dual slope path loss model in which square law path loss is assumed for distances less than 50 m and a fourth-order path loss law is assumed for distances greater than 50 m, as shown in the following equation.

$$
\begin{aligned}
Path\ loss &= \begin{cases} K + 20\log_{10}(d/d_0) & d \le d_c \\ K + 20\log_{10}(d_c/d_0) + 40\log_{10}(d/d_c) & d > d_c \end{cases} \\
K &= free\ space\ loss\ at\ d_0 = 32.5 + 20\log_{10}(f) + 20\log_{10}(d_0) \\
d_0 &= 1m \\
d_c &= 50m
\end{aligned}
$$

where *d* is the distance between the devices in metres and the *f* is the operating frequency in GHz.

The results of the calculations for the first scenario (in which the interferer is a TDD LTE UE) are presented in Table 10, which shows the wanted ZigBee signal, assuming a level of 20 dB above MUS, the required C/I to achieve a PER of <1% and the MCL and the MSD calculated using the assumptions outlined above. The results indicate that the MCL and MSD increase as the MUS of the device decreases, eg, Device 4 has the lowest MUS and it has the greatest MSD. The results also demonstrate that the MCL and MSD increase for the 20 MHz TDD LTE interferer compared with the 10 MHz TDD LTE interferer. This is consistent with the observation that the wider bandwidth signal causes a greater degradation in the ZigBee link performance.

Device	10MHz TDD LTE Interferer				20MHz TDD LTE Interferer			
	Wanted Signal (dBm)	Required C/I (dB)	MCL (dB)	MSD (m)	Wanted Signal (dBm)	Required C/I (dB)	MCL (dB)	MSD (m)
1	-72.1	-53.1	44.1	1.6	-72.1	-46.7	50.5	3.3
2	-75.25	-52.3	48.1	2.5	-75.25	-47.7	52.7	4.2
3	-70.8	-52.7	43.2	1.4	-70.8	-46.9	49.0	2.8
4	-79.65	-52.7	52.1	4.0	-79.65	-46.7	58.1	7.9

Table 10   Results of minimum coupling loss calculations when a TDD LTE UE is considered as the source of interference assuming received ZigBee signal is at MUS + 20dB.

Similarly, the results for the second case (where a TDD LTE BS is the source of interference) are shown in Table 11. These results show trends similar to those observed in the first scenario, ie, the device with the lowest MUS (Device 4) requires the largest MSD and also that a larger MSD is required for the 20 MHz TDD LTE interferer compared with the 10 MHZ TDD LTE interferer.

Device	10MHz TDD LTE Interferer				20MHz TDD LTE Interferer			
	Wanted Signal (dBm)	Required C/I (dB)	MCL (dB)	MSD (m)	Wanted Signal (dBm)	Required C/I (dB)	MCL (dB)	MSD (m)
1	-72.1	-52.1	86.1	99.9	-72.1	-46.7	94.5	161.9
2	-75.25	-52.9	88.5	114.3	-75.25	-47.6	96.8	184.3
3	-70.8	-51.9	85.0	93.7	-70.8	-46.0	93.9	156.4
4	-79.65	-52.0	93.8	155.2	-79.65	-46.7	102.0	250.0

Table 11   Results for minimum coupling loss calculations when a TDD LTE BS is considered as the source of interference assuming received ZigBee signal is at MUS + 20dB.

It should be noted that, although the results presented in Table 10 and Table 11 provide a reasonable indication of the MCL and MSD values that may be required in some applications, there may be other applications in which much lower values could be tolerated without a noticeable degradation in the performance of the system from the user's perspective. For example, when acknowledgement and retransmissions are enabled within the ZigBee system, then the impact of increasing the interference levels will be to decrease the throughput, rather than increase the overall error rate. In applications that are resilient to increased data latency (eg, smart meters), then smaller MCL and MSD values could be tolerated. The impact of acknowledgements and retransmissions on the ZigBee system is investigated in the next section.

10 Protocol Test Results and Analysis

The results presented in the previous section were generated with packet acknowledgements and retransmissions disabled to provide a 'raw' measure of the PER. In order to understand the capabilities of the ZigBee protocol stack to combat the effects of link errors, a set of measurements was performed with the packet acknowledgment and retransmission functionality associated with the ZigBee protocol enabled. Device 1 was used for the purposes of these tests, as it provides a simple interface to enable or disable various features

in the protocol stack. For the duration of these tests, the maximum number of re-transmissions permitted for each packet was set to three.

Figure 20 shows the performance of Device 1 in the absence of any interference. The *x*-axis shows the received ZigBee signal power relative to the measured MUS of Device 1.The blue line shows the net data rate, or throughput, (in kb/s) achieved by the device when packet acknowledgments and retransmissions were enabled. As the ZigBee signal power is increased and more packets arrive uncorrupted at the receiver without the need for retransmission, the data rate across the ZigBee link increases, and reaches a peak value of approximately 55 kb/s as the MUS value is approached. At all measurement points shown in the figure, the PER was 0%, ie, there was no packet loss with acknowledgements and retransmissions enabled. The peak data rate of 55 kb/s is compared with a data rate of 153kb/s which is achieved at the MUS level when retransmissions and acknowledgements are not enabled. In order to understand the reasons for this drop in data rate, the throughput was measured with acknowledgements enabled, but retransmissions disabled, and the result was 99 kb/s. Therefore, we conclude that the throughput drops by around one third as a result of the additional transmission delay introduced as the transmitter waits for the acknowledgement of successfully transmitted packets. When retransmissions are also enabled, the throughput decreases by a further 50%, to 55 kb/s, and this appears to be a result of the introduction of the carrier sense multiple access-collision avoidance (CSMA-CA) mechanism, which is also used when retransmissions are enabled on this device. CSMA-CA introduces a random 'back-off' period before the ZigBee transmitter performs a clear channel assessment (CCA) of the ZigBee channel to determine whether it is clear to transmit and this additional delay decreases the overall throughput.

The green curve in the figure shows the PER performance of the device as the received signal strength is varied for the case when packet acknowledgments and retransmissions are disabled. Together, these two curves demonstrate the trade off between PER performance and data throughput in the absence of interference. For example, with a received ZigBee signal that is 2 dB below the MUS level, the resulting PER without acknowledgements and retransmissions is around 10% and the throughput is around 135 kb/s (ie, the transmission rate is 153 kb/s, but 10% of these transmitted packets are lost, decreasing the throughput by 10%). If acknowledgements and retransmissions are switched on at this same received signal strength, the PER will fall to 0%, but the throughput drops to around 52 kb/s.
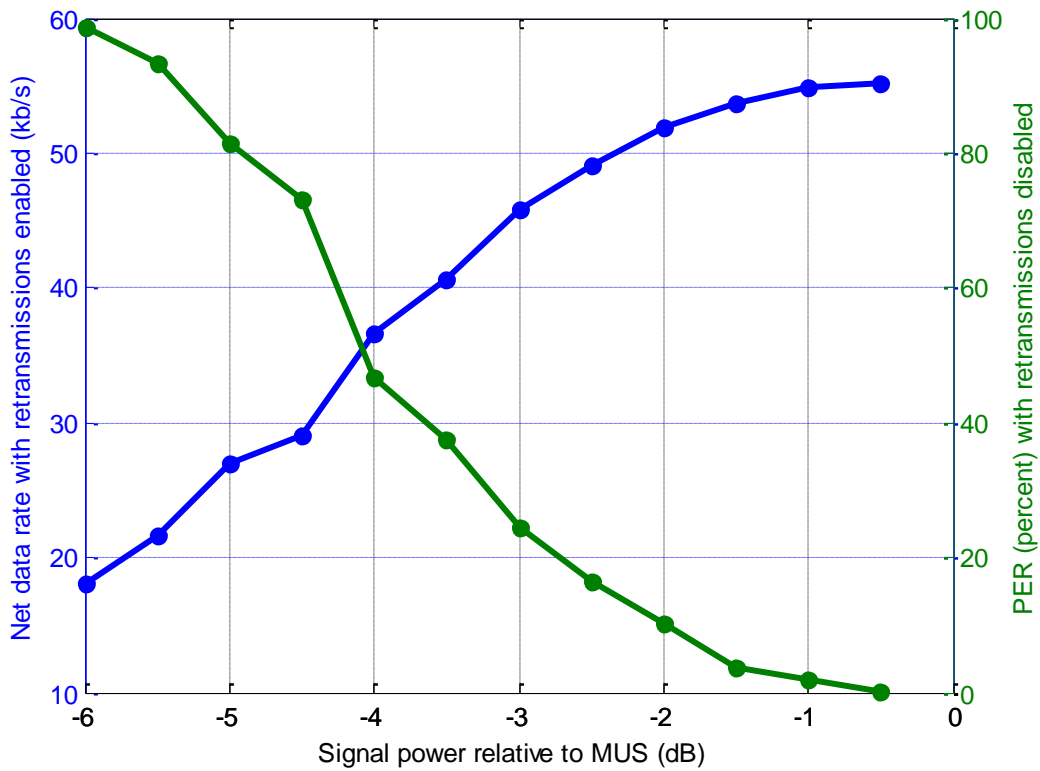
Figure 20   Data rate as a function of transmit power with frame retransmission enabled. The packet error rate when retransmissions are disabled is also plotted for comparison.

Figure 21 shows the results of protocol tests in the presence of a co-channel 10 MHz downlink TDD LTE interferer with the ZigBee signal level 20 dB above MUS. The green curve (showing the PER in the absence of packet acknowledgments and retransmissions) corresponds with our earlier results (see Figure 12) showing a target C/I of approximately 2.5 dB for a PER of <1%. With acknowledgements and retransmissions enabled, the net data rate (blue curve) increases from 28 kb/s to 55.5 kb/s as the C/I is increased from -3.5 dB to 2.5 dB.
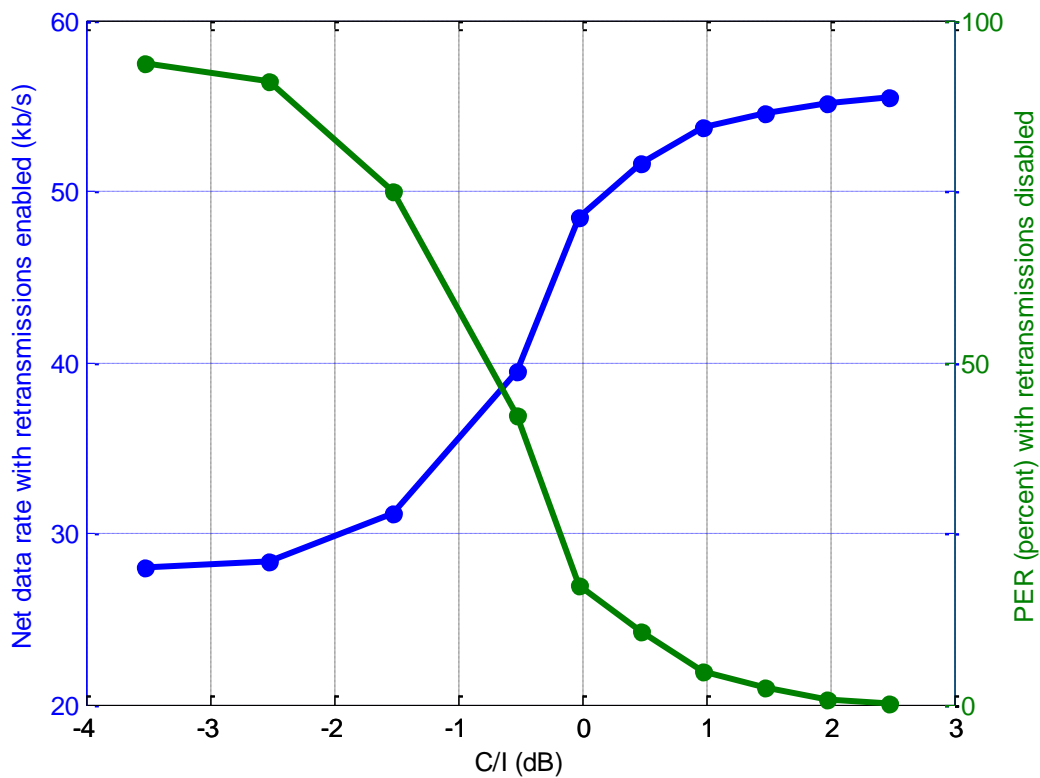
Figure 21 Net data rate as a function of C/I with frame retransmissions enabled in the presence of 10 MHz downlink TDD LTE interference. Also shown is the PER with retransmissions disabled. The ZigBee signal level was 20 dB above MUS.

The effect of changing the LTE frame configuration on the net data rate achieved by Device 1 is shown in Figure 22. This figure shows the net data rate as a function of C/I in the presence of a 10 MHz downlink TDD LTE interferer and with the ZigBee signal level at 20 dB above MUS. The red curve shows the results for LTE Frame Configuration 1 (four out of ten slots reserved for the downlink) and the blue curve for LTE Frame Configuration 5 (eight out of ten slots reserved for the downlink). As expected, the performance is slightly better when Frame Configuration 1 is used, as the number of vacant TDD slots is higher, allowing more packets (and retransmissions) to succeed. Once the C/I ratio is sufficiently high (ie, 2 dB or higher), the choice of frame configuration becomes irrelevant, and both converge at a peak value of about 55 kb/s. The difference in performance is much greater at low values of C/I where the PER is higher.
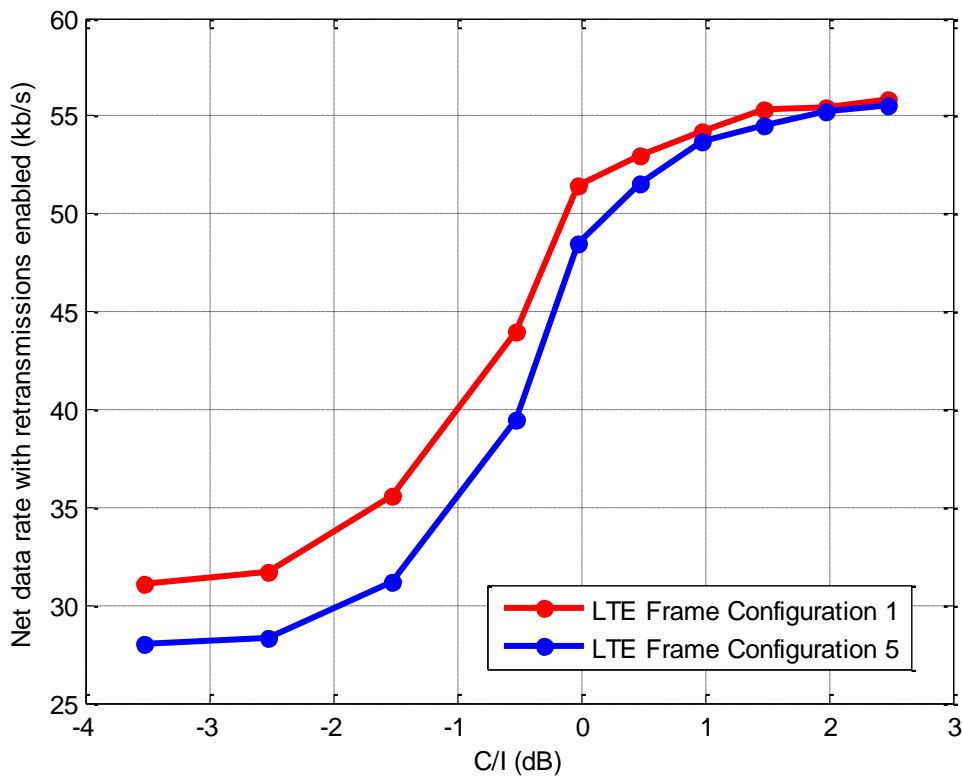
Figure 22   Comparison of net data rate achieved by Device 1 in the presence of 10 MHz downlink LTE interferers with two different frame configurations. The ZigBee signal level was 20 dB above MUS.

11 ZigBee Application Testing

As the final part of this study, a set of ZigBee home automation products was tested and the effects on the system performance were observed when operating in the presence of a TDD LTE interferer. The purpose of these tests was to investigate whether the communication link between nodes in an off-the-shelf ZigBee-based system can cope with the presence of a TDD LTE UE in its vicinity when operating in a typical indoor deployment scenario.

The end-user equipment used in these tests comprised a central control unit, a mains relay and a remote control. A system diagram of the test set up is shown in Figure 23. The tests involved controlling the mains relay by sending commands from the remote control in the presence of TDD LTE interference. The tests were performed for both 10 MHz and 20 MHz TDD LTE uplink interferers with Frame Configuration 3 (ie, the same configuration as that used for generating uplink interference in the LTE OOBE tests described in Section 6.3.2).

The mean transmit power level was set to 23 dBm for the 10 MHz interferer, but it had to be limited to 22 dBm for the 20 MHz interferer so as not to exceed the maximum peak envelope power (PEP) value allowed on the signal generator.
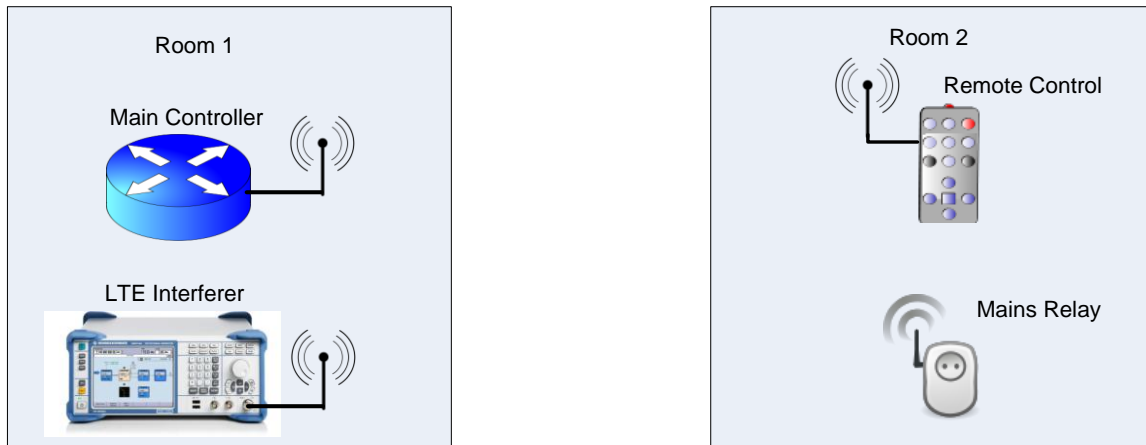
Figure 23   An example of test set up for ZigBee application testing. This particular example illustrates the positioning of equipment for Test Scenario 2 specified in Table 12.

Table 12 shows the combinations of equipment locations for which these tests were performed. The relay and main controller were placed in two separate rooms ('Room 1' and 'Room 2') at the opposite ends of MAC Ltd's premises, resulting in a separation of approximately 32 m between them. The location of the LTE interferer and the remote control was changed, as shown in the table.

Test Scenario	Equipment Location (Room Number)			
	LTE Interferer	**Main Controller**	**Mains Relay**	**Remote Control**
1	1			1
2	1	1	2	2
3	2			1
4	2			2

Table 12   Test scenarios for ZigBee end-user equipment testing.

In each of the four scenarios listed above, the tests were performed using two types of TDD LTE interferers: a 10 MHz uplink interferer located at 2385 MHz and a 20 MHz uplink interferer located at 2380 MHz. In Scenarios 1 and 2, the LTE interferer was located in the same room as the main controller at a distance of approximately 50 cm. These scenarios represent the case when the interferer is located very close to the main controller of a ZigBee

network. Similarly, Scenarios 3 and 4 represent the situation where the interferer is located close to an end node. Again, the separation between the interferer and the switch was approximately 50 cm in the last two scenarios.

The ZigBee equipment was found to work reliably in all four scenarios listed above. The switching operation was performed a number of times for each scenario and the switch always responded correctly to the commands sent by the remote control. Therefore, in the test scenarios listed above, there was no noticeable impact of introducing a TDD LTE uplink interferer operating at a frequency close to the lower edge of the 2.4 GHz ISM band.

12 Conclusions

In this study, the effect of interference from TDD LTE equipment operating in the 2.3 GHz to 2.4 GHz band on the operation of a number of ZigBee devices was measured. The main set of tests was performed on five devices (based on chipsets from four different vendors) that were chosen as a representative sample of ZigBee chipsets available in the market. These tests involved measuring the target C/I (the C/I needed to maintain a PER of less than 1%) of the ZigBee devices when operating in the presence of a TDD LTE or CW interferer. The procedure used for these tests involved measuring the PER on a ZigBee transmission link in the presence of interference. The ZigBee devices were set to transmit at Channel 11 (centred at 2405 MHz), whereas the LTE signal was centred at a range of test frequencies and the target C/I was measured at each of the test frequencies.

The measurement results for these tests have been presented in the preceding sections of this document. The devices tested in this study can be divided into two groups based on their behaviour in the presence of interference. Device 1 displayed signs of non-linear behaviour at frequency offsets greater than -15 MHz between the centre frequencies of the wanted ZigBee and LTE interference signals. The performance of Device 1 at large frequency offsets is much poorer in the presence of LTE interference compared to CW interference. Device 3 also shows a similar behaviour and its performance in the presence of LTE interference is much worse compared to CW interference. This suggests that these devices are operating in their non-linear regions and the wideband LTE signal is producing in-band signal components through intermodulation effects. Devices 2 and 4 belong to the second group, in which the target C/I levels at large frequency offsets (greater than -35 MHz) are identical, irrespective of the interference type. This suggests that these devices continue to operate in their linear

region at these interference levels and the dominant interference mechanism is the blocking (or desensitisation) of receiver due to the level of interference entering the receive chain. The results for Device 5 were inconclusive in this regard, but we would expect it to perform in the same way to Device 4, since they are based on the same chipset. The minimum separation distance (MSD) between the ZigBee devices operating at the lowest frequency channel (2405 MHz) and a TDD LTE UE operating at the highest planned channel (ie, 2385 MHz and 2380 MHz for 10 MHz and 20 MHz TDD LTE signals, respectively) was found to vary among the ZigBee development boards tested in this study. The MSD varied from 1.4 to 4.0 metres in the case of 10 MHz TDD LTE interference, and from 2.8 to 7.9 metres for 20 MHz TDD LTE interference. Similar trends were observed when a TDD LTE BS was considered as the source of interference. In this case, the MSD varied from 93.7 to 155.2 metres in the case of 10 MHz TDD LTE interference, and from 156.4 to 250.0 metres for 20 MHz TDD LTE interference. In both cases, the ZigBee devices having the lowest MUS required the highest MSD.

We found that the reliability of a ZigBee link can be improved by enabling the mechanisms such as frame acknowledgment and retransmission and CSMA-CA at the expense of a decrease in the net data rate achieved by the link.

Finally, we tested the operation of a ZigBee-based home automation system in the presence of TDD LTE interference centred at the planned channels closest to the ISM band. These products comprised a central controller, a mains relay, and a remote control. We found that the presence of the TDD LTE UE interference had no measurable impact on the operation of these devices.

Our overall conclusion is that the operation of TDD LTE equipment in the vicinity of the 2.4 GHz ISM band is unlikely to cause significant disruption to the operation of typical ZigBee devices available in the market in low data rate, non real time applications where the ZigBee system is operating at a significant margin (eg, >20dB) above its own specific minimum useable sensitivity. Although the 'raw' performance of the ZigBee link could be adversely affected when the separation between ZigBee and TDD LTE UE equipment is less than a few metres, this is likely to be overcome by mechanisms such as frame retransmission and CSMA-CA. However, system performance issues could arise if the ZigBee equipment is operated in close proximity to a high power TDD LTE BS.

References

1. ZigBee Alliance, 'ZigBee Specification', Document Number 053474, Release 17, 17 January 2008

2. IEEE Computer Society, 'IEEE Standard for Information Technology – Telecommunications and Information Exchange between Systems – Local and Metropolitan Area Networks – Specific Requirements – Part 15.4: Wireless Medium Access Control (MAC) and Physical Layer (PHY) Specifications for Low Rate Wireless Personal Area Networks (WPANs), IEEE std. 802.15.4-2003.

3. Ofcom, 'UK Frequency Allocation Table 2013', Issue No. 17, Feb 2013, available at http://stakeholders.ofcom.org.uk/binaries/spectrum/spectrum-information/UKFAT_2013.pdf

4. ZigBee Alliance, 'ZigBee IP Specification', ZigBee Public Document 13-002r00, February 2013.

5. ZigBee Alliance, 'ZigBee RF4CE Specification', ZigBee Document 094945, Version 1.01, January 2010.

6. Texas Instruments, 'CC2430 data sheet', February 2011, available at http://focus.ti.com/lit/ds/symlink/cc2530.pdf.

7. Freescale Semiconductor, 'MC1322x Technical Data', Rev. 1.3, Oct 2010, available at http://www.freescale.com/files/rf_if/doc/data_sheet/MC1322x.pdf.

8. Silicon Labs, 'EM351/EM357 data sheet', 120-035X-000 Rev. 1.2 Final, available at http://www.silabs.com/Support%20Documents/TechnicalDocs/EM35x.pdf.

9. Atmel, 'AT86RF233 data sheet', Rev. 8351C–MCU Wireless–02/13, Feb 2013, available at http://www.atmel.com/Images/Atmel-8351-MCU_Wireless-AT86RF233_Datasheet.pdf

10. 3GPP, 'Evolved Universal Terrestrial Radio Access (E-UTRA); User Equipment (UE) radio transmission and reception', 3GPP TS 36.101 version 11.3.0 Release 11.

11. Ofcom Research Document, 'LTE User Equipment Coexistence with 862 – 870 MHz', 11 September 2012

12. Rohde and Schwarz, 'R&S SMBV 100A Vector Signal Generator, Specifications', Test and Measurement Data Sheet 04.0, April 2013 (available at www.rohde-schwarz.com, accessed on 12 June 2013).

13. Vaunix Technology Corporation, http://vaunix.com/products/digital-attenuator/overview.cfm, accessed on 03 June 2013.

14　Antenova M2M, 'M2M Rufa 2.4 GHz SMD Antenna Part No. A5839 / A5887', Product Specification AE020157-O, Release Date 8 Feb 2013 (available at http://www.antenova-m2m.com, accessed 4 Jun 2013).

15　Linx Technologies, 'Ultra Compact Chip Antenna Data Guide - ANT-2.4-CHP-x, ANT-868-CHP-x, ANT-916-CHP-x', 2009 (available at　https://www.linxtechnologies.com, accessed 4 Jun 2013).

16　Rainsun, 'AN1003 Multilayer Chip Antenna', Data Sheet, Jun 2006 (available at www.rainsun.com, accessed 4 Jun 2013).